PREPARATION OF LAYERED INTERCALATION COMPOUNDS VIA ONE-POT *IN*

SITU SYNTHESIS

THESIS

Presented to the Graduate Council of
Texas State University-San Marcos
in Partial Fulfillment
of the Requirements

for the Degree

Master of SCIENCE

By

Lichen Xiang, B.S.

San Marcos, Texas

December 2012

PREPARATION OF LAYERED INTERCALATION COMPOUNDS VIA ONE-POT *IN*

SITU SYNTHESIS

Committee Members Approved:

_____

Luyi Sun, Chair

_____

Benjamin R. Martin

_____

Clois E. Powell

Approved:

_____

J. Michael Willoughby
Dean of the Graduate College

COPYRIGHT

by

Lichen Xiang

2012

FAIR USE AND AUTHOR'S PERMISSION STATEMENT

Fair Use

Duplication Permission

ACKNOWLEDGEMENTS

TABLE OF CONTENT

LIST OF TABLES

LIST OF FIGURES

xi

ABSTRACT

PREPARATION OF LAYERED INTERCALATION COMPOUNDS VIA ONE-POT *IN*

SITU SYNTHESIS

by

Lichen Xiang, B.S.

Texas State University-San Marcos

December 2012

SUPERVISING PROFESSOR: DR. LUYI SUN

Layered materials, such as layered silicates, layered phosphates, layered double hydroxides, and metal chalcogenides, have attracted highresearch interest in the past few decades. Layered materials have been widely used in our daily life, such as batteries, catalysts, medical devices, waste treatment, and lubricants. A wide range of chemicals, including small molecules, oligomers, polymers, biomolecules, and ions, have been intercalated into layered materials for new or enhanced properties. Various approaches

have been developed to achieve intercalation were reviewed in this thesis. Nanostructured organic-inorganic hybrid materials, including polymer nanocomposites, layer-by-layer assembled thin films, have been extensively investigated over the past two decades and have found wide applications owing to their excellent performance. Either regular polymer nanocomposites or layer-by-layer assembled thin films are typically prepared using pre-synthesized nanofillers/nanoplatelets. Here, we report a new approach to prepare nanostructured hybrid materials via in situ synthesis of nanoplatelets within the polymer/monomer matrix. Alpha-zirconium phosphate (ZrP) was synthesized in a solution system containing a polymer (such as polyethylene glycol, PEG) or monomer (such as acrylamide). In the case of polymer in situ synthesis, during the synthesis of ZrP, PEG chains were embedded into the ZrP interlayer space, leading to a larger interlayer distance, which is similar to the intercalated layered compound. Proper formulation ratio proved to be critical to avoid forming pristine ZrP, and avoid interfering the growth of the layered structure of ZrP. It has also been found that longer polymer chains are desirable for minimizing the formation of pristine ZrP, but would not affect the interlayer distance. All the PEG chains are perfectly parallel to the layer planes. Besides polymers, monomer molecules (such as acrylamide) have also been successfully embedded into the interlayer space to form an intercalated structure during in situ synthesis. The monomer molecules were further polymerized in the ZrP layer galleries. As a result, the inorganic/organic hybrid intercalation compound was synthesized without pre-form either layered host materials or guest species.

CHAPTER I

INTRODUCTION FOR METHODOLOGY OF INTERCALATION

1. Introduction

Inorganic-organic hybrids, particularly the ones with an intercalated structure, have attracted substantial attention, because they can potentially bring unique properties combining distinct features of organic and inorganic components within a single molecular composite.[1] In addition, new or enhanced phenomena can also arise as a result of the interface between the inorganic and organic components.[2] While a wide range of intercalated structures exist, the vast majority ones are based on 2-dimensional (2-D) layered materials.[3] In the past few decades, the understanding of intercalation chemistry has been significantly advanced,[1a] and intercalation materials have also been well developed due to their extraordinary importance and wide applications in batteries,[1a, 4] fuel cells,[5] biomedical devices,[6] catalysis,[1a, 7] display systems,[1a] nuclear waste treatment,[8] etc.

The phenomenon of intercalation was first discovered ca. 600-700 A.D. in China.[9] At that time, Chinese intercalated alkali metal ions into natural minerals such as kaolin, etc. to make porcelain.[10] In 1840, Schafhäutl described the first intercalation phenomenon in the literature,[11] in which they tried to dissolve graphite in sulphuric acid, the result is that the graphite cannot dissolve but the graphite layers were swelled.[11] The modern intercalation research started from a paper in 1926 by Fredenhagen et al., in

which they reported the uptake of potassium vapor into graphite.[12] Since then, intercalation reactions have fascinated chemists and materials scientist. Many approaches to achieve intercalation have been developed, and widespread application of intercalation compounds has been explored.

So far, various approaches to achieve intercalation have been developed based on different reaction/interaction mechanisms.[1] Meanwhile, intercalations have been carried out at various interfaces, including solid-solid, solid-liquid, and solid-gas interfaces.[1] While it is always preferable to achieve direct intercalation via one-step reaction, some guest species are difficult or impossible to be directly intercalated owing to size mismatch and/or lack of driving force. To solve such issues, a series of approaches have been developed, including multi-step intercalation (based on pre-intercalation to increase interlayer distance), exfoliation-reassembly, and layer-by-layer self-assembly.[1a] As such, it is very important to summarize major intercalation methods. Overviewing the intercalation mechanisms and methodologies helps researchers in the field to choose an appropriate approach to achieve intercalation. In addition, it facilitates to develop new intercalation methodology based on the earlier work.

While intercalation in 3-dimentional (3-D) framework and 1-dimensional (1-D) linear chain lattices have also been explored, 2-D layered materials have dominated intercalation research.[1b, 3] Therefore, this review will focus on the intercalation of 2-D layered compounds. 2-D layered materials have a similar overall structure, mainly differing in the sheet composition and unit structure. They are characterized by strong intralayer covalent bonding and weak interlayer interactions. The layers may be electrically neutral, or positively, or negatively charged. For neutral layered compounds,

including graphite, metal chalcogenides, metal oxides, metal halides, their layers are held together via van der Waals force, and their interlayer space is a connected network of empty lattice sites. For positively charged (such as layered double hydroxides) or negatively charged (including metal phosphates and phosphonates, semectite clays and silicates, silicides) layers, they are held together by weak electrostatic forces and their interlayer spaces are filled by counter ions or a combination of ions and solvent molecules (such as water).

2. Intercalation mechanisms

Most of the intercalations rely on the reactions/interactions between the guest species and host layered materials, including ion-exchange, acid-base reaction, hydrogen bonding, redox reaction, and electrochemical reaction,[1, 13] which will be reviewed below. These reactions/interactions are able to generate a driving force, which provides energy to drive the guest compounds into the galleries. Typically, a higher pressure and/or a higher temperature would expedite the intercalation reactions and increase the degree of intercalation. In addition, some assisting means, such as ultrasonication and microwave radiation are also widely used to promote the intercalation.

2.1 Ion-exchange intercalation

Ion exchange intercalation theory has been well developed so far. As discussed above, many host materials contain ion between the layers. As a result, intercalation reactions can occur through the ion-exchange process between the guest ions and interlayer exchangeable ions.

Ion exchange intercalation needs to accord with the following conditions: First, the interactions of the neighboring layers must be weaker than the interaction of the guest compound with the host layers.[14] As a result, the layer surfaces turn to be intercalating active sites to be able to generate intercalation with the guest species. Second, the layers need to spread apart to accommodate the guest molecules. Thus, the layer distance normally will be increased, as shows in Figure 1. [14]
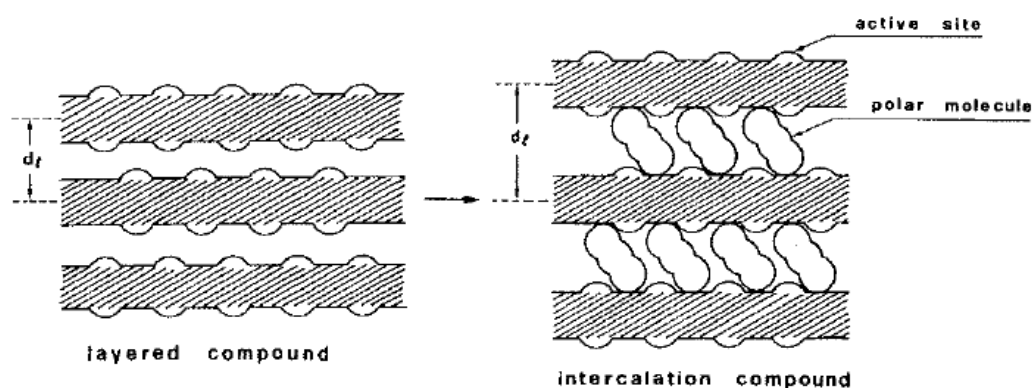
Figure 1. Schematic illustration of the intercalation of polar molecules between the layered sheets.[14]

LDH is one of the most commonly used 2-D layered hosts.[15] The general formula of LDH is $[M(II)_{1-x}M(III)_x(OH)_2][A_{x/n}\cdot mH_2O]$, where M(II) cations are typically Mg, Zn, Cu, Co, or Ni, and M(III) cations are usually Al, Fe, Cr, or Ga. A is an exchangeable anion.[16] Figure 2[16] shows a typical structure of LDHs. The exchangeable anions exist between metal octahedral layers. During the ion exchange reaction, guest ions replace the interlayer ions.
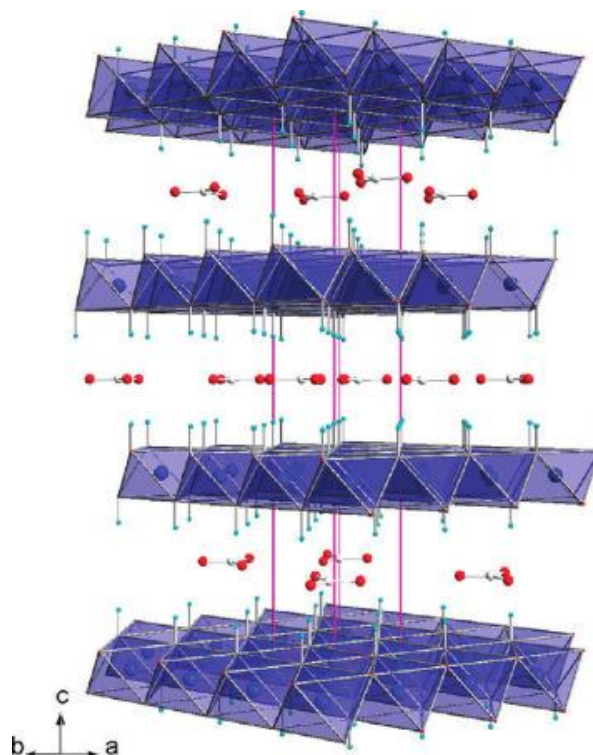
Figure 2. Typical structure of LDHs.[16]

Bastianini et al. intercalated iodine-iodide into LDHs to make a dye sensitized solar cell, representing a typical example of ion exchange intercalation.[16] In this experiment, Zn/Al=2/1 LDH was used as the host synthesized via the urea method. The primary product ZnAl-CO_3 was first titrated by HCl solution, undergoing an ion exchange process, to obtain ZnAl-Cl LDH. Pre-formed ZnAl-Cl LDH were then reacted with potassium iodide solution under stirring for 24 hours. The final product with formula $[Zn_{0.61}Al_{0.39}(OH)_2](Cl)_{0.17}I_{0.22}\cdot0.34H_2O$ was further washed a couple times and dried. Their X-ray diffraction (XRD) patterns in Figure 3 suggest that after the ZnAl-CO_3 (pattern a) LDH was exchanged with Cl^-, its interlayer distance was increased from 7.56Å to 7.74Å (pattern b). After I^- anions replaced Cl^-, ZnAl-I possessed an even larger interlayer distance of 8.10Å (pattern c).
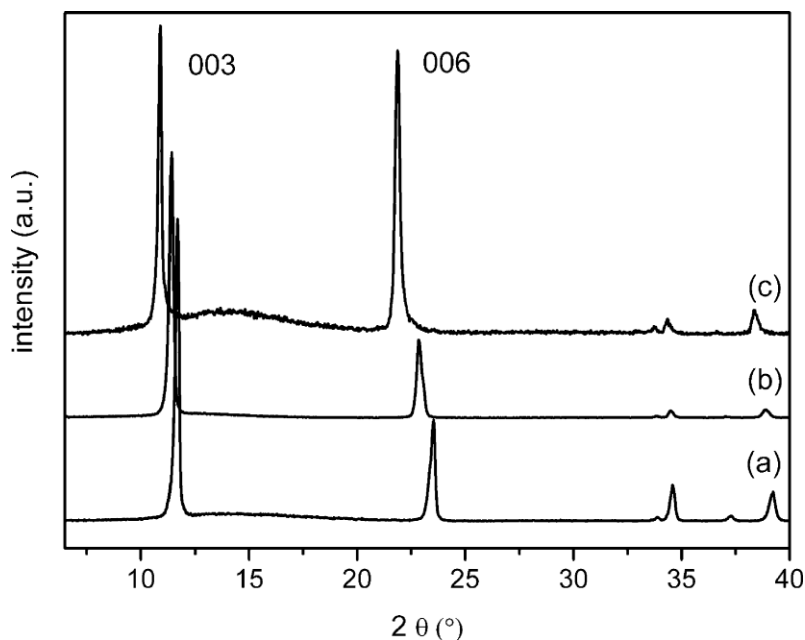
Figure 3. XRD patterns of ZnAl-CO_3 (a); ZnAl-Cl(b); ZnAl-I(c).[16]

While in most cases the interlayer distance will be increased after intercalation as discussed above, in some cases, after the guest species were exchanged into galleries, the interaction between layer sheets turns to be stronger. As a result, the guest species enables the layer sheets to pack closer than it originally was.[17]

Smectite clays possess exchangeable cations in the galleries, which can be intercalated via cation exchange reactions.[18] Figure 4 shows a scheme of 2:1 layer smectite clay, which is composed of an octahedral Al2O3 layer sandwiched by two tetrahedral SiO2 layers. Some of the Al^{3+} in the octahedral layers are replaced by other cations such as Mg^{2+}, or Fe^{3+}.[18] Montmorillonite (MMT) belongs to 2:1 smectite clays group. Each layer of MMT is negative charged. In these galleries, cations such as Mg^{2+}, Na^+, and Ca^{2+} balance the negative charges. These interlayer cations can be replaced easily by positively charged organic or inorganic guests via cation exchange process. In

an example of intercalating glycine ethylester (Gly) into MMT, Na-MMT was chosen as the guest material. After mixed with Gly in liquid phase under stirring, Gly was intercalated into the galleries via an ion exchange process.[17] Part of Gly-MMT was further intercalated with Gly to make Gly-Gly-MMT intercalation compound. The XRD pattern in Figure 5[17] shows differences before and after intercalation. After intercalation of Gly, the interlayer distance of MMT did not increase but reduced. Most intercalation processes lead to an increase in interlayer space, but in this case, the intercalation compounds containing both monolayered Gly-MMT (12.7Å) and bilayered Gly-Gly-MMT (13.3Å) possessed a lower interlayer space than the original host Na-MMT (15.1Å). This was because of the enhanced interactions between layers by Gly. Similar phenomena were observed for ethylene diammonium intercalation compound[19] and alkylammonium intercalation compound.[20]
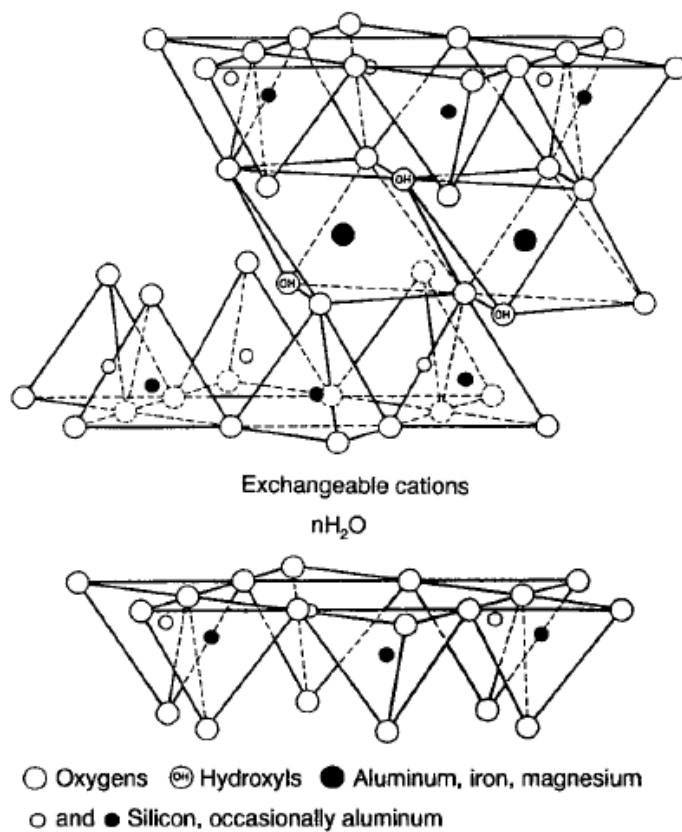
Figure 4. Scheme structure of 2:1 smectite molecule.[18]
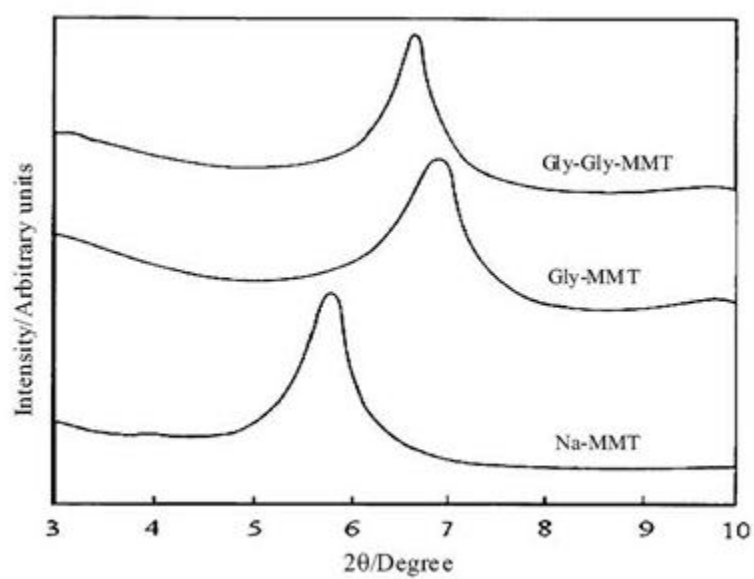
Figure 5. XRD patterns of Gly-Gly-MMT, Gly-MMT and Na-MMT[17].

2.2 Redox intercalation reaction

In late 1970s, Palvadeau et al. succeeded to intercalate lithium ion into FeOCl lattice galleries.[21] In their experiment, the guest species lithium was pre-dissolved in aqueous ammonia. The intercalation reaction occurred via the NH_2^- ions substitution of Cl^-, during which Fe^{3+} was reduced to Fe^{2+}.[11] The intercalation reaction via redox reaction to generate driving force to push the guest materials into the layered galleries called redox intercalation.

One of the most typical examples to explain redox intercalation method is intercalation of alkali metals into $2H-TaS_2$:

$$A + Ta^{4+}S_2 \rightarrow A^+Ta^{3+}S_2 \quad (A= \text{alkali metal}) \tag{1}$$
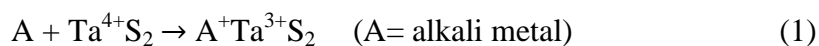
In this reaction, electron transfer from alkali metal to Ta^{4+} to form A^+ and Ta^{3+}. This reaction generates the driving force to increase the bond strength of A-S over A-A to force intercalation reaction to complete.

Another typical example for redox intercalation is $VOPO_4 \cdot 2H_2O$, if a proper reducing agent is present, cations are able to intercalate into $VOPO_4 \cdot 2H_2O$ layers via redox intercalation reaction. Normally, the good reducing agents such as I^-, $S_2O_3^{2-}$, SO_2, etc. will "help" metal cations (e.g. Li^+, Na^+, K^+, Mg^{2+}, Zn^{2+}, etc.) to intercalate into $VOPO_4 \cdot 2H_2O$ via redox reaction.[22] For example, when $VOPO_4 \cdot 2H_2O$ reacts with KI, the reaction equation is:

$$2V^VOPO_4 \cdot 2H_2O + 2xKI \rightarrow 2K_x V^{IV}_x V^V_{1-x}OPO_4 \cdot 2H_2O + xI^2 \tag{2}$$
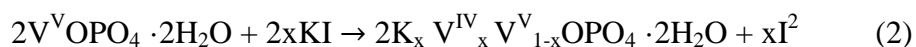
The reaction is normally rapid and spontaneous at room temperature. The intercalant normally co-intercalants with H_2O molecules into the galleries.[22]

2.3 Interaction assisted by hydrogen bonding

While ion-exchange and redox reactions have been the major mechanisms for intercalation, sometime a second mechanism may exist to promote the intercalation to a much more significant extent.

Lin and coworkers discovered an interesting phenomenon that when they tried to intercalate a large amount of poly(oxypropylene) 400-sebacic acid (POP400-SA) into the montmorillonite (MMT) or fluorinated mica (Mica). It was observed that the layered distance kept increasing with an increasing amount of guest species.[23] They found that the initial driving force that enabled POP400-SA to insert into the layered host was ion-exchange reaction. However, when they continually added more guest species which was several times more than the cation exchange capacity of the host, the interlayer distance still kept increasing, which suggested that a second driving force might exist to force the guest species into the galleries. It was later identified that the driving force that caused intercalants to aggregate is the hydrogen bonding between the amide groups and POP back bone hydrophobic effect.

Table 1[23] illustrates the XRD and TGA results for different intercalants, where POP400, POP2000, and POP4000 represent POP with different molecular weights; AA and SA were referred to as adipic acid and sebacic acid, respectively. As the result shown in Table 1[23], for POP2000, with an increase of the intercalant from 1:1 ratio to 2:1 ratio, the layer distance (d spacing) exhibited a marginal increase, from 5.7 to 5.8 nm in

MMT and 3.8 to 4.0 nm in Mica. For POP400AA, there was virtually no d spacing

variation between 1:1 ratio and 2:1 ratio. In comparison, in the case of POP400-SA, as

the increase of guest to host ratio from 1:1 to 4:1, the d spacing was dramatically

increased from 2.0 to 7.1 nm for MMT and 1.8 to 7.8 nm for Mica. These phenomena can

be well explained by Figure 6[23]. As illustrated in Figure 6(a)[23], the hydrophobic effect

between the backbones of POP2000 chains force the POP chains to align vertically or

semi-vertically between the layers. However, since POP2000 does not have amide

hydrogen bonding interaction, when the cation exchange capacity is full, there is no

driving force to lead more POP2000 guests to intercalate into the galleries. For the case

of hydrophilic sample POP400-AA, the hydrophobic interactions do not exist between

the POP back bones. Meanwhile, the hydrogen bonding of amide will be more ready to

react with layer surfaces instead of giving a driving force for excessive POP400-AA

guests. As a result, the POP400-AA chains in between the galleries laid on the layer

sheets and no hydrogen bonding driving force will lead to excessive intercalations. For

POP400-SA, it has both hydrophobic effects and hydrogen bonding between the confined

POP400-SAs. Because of the hydrophobic effect, POP400-SA chains between the

galleries will vertically aligned. But meanwhile, it gives amide hydrogen bonding

reaction more chance to attract excess POP400-SA molecules rather than react with

cations on the surface of layered sheets. The combination of the two mechanisms led to a

significant increase of the interlayer distance.

This interesting discover of using hydrogen bonding interactions to drive intercalant

into layered galleries gives us a new perspective for intercalating large molecules,

particularly large bio-molecules which can be hydrogen bonded. Hydrogen bonding

reaction intercalation method may be more extensively explored in the future.

Table 1. XRD and TGA result for different POP intercalant in different ratio.

Intercalating agent	Equivalent ratio	d spacing by XRD(nm)		Organic fraction by TGA (w/w)	
		MMT	Mica	MMT	Mica
None	-	1.2	1.2	-	-
POP400	1/1	1.9	1.7	26/74	22/78
POP2000	1/1	5.7	3.8	63/37	49/51
	2/1	5.8	4.0	68/32	55/45
POP4000	1/1	9.2	6.8	72/28	66/34
POP400-AA	1/1	-	1.7	-	27/73
	2/1	-	1.7	-	30/70
POP400-SA	1/1	2.0	1.8	52/48	47/53
	2/1	5.2	5.8	62/38	58/42
	3/1	6.6	7.0	72/28	65/35
	4/1	7.1	7.8	73/27	70/30
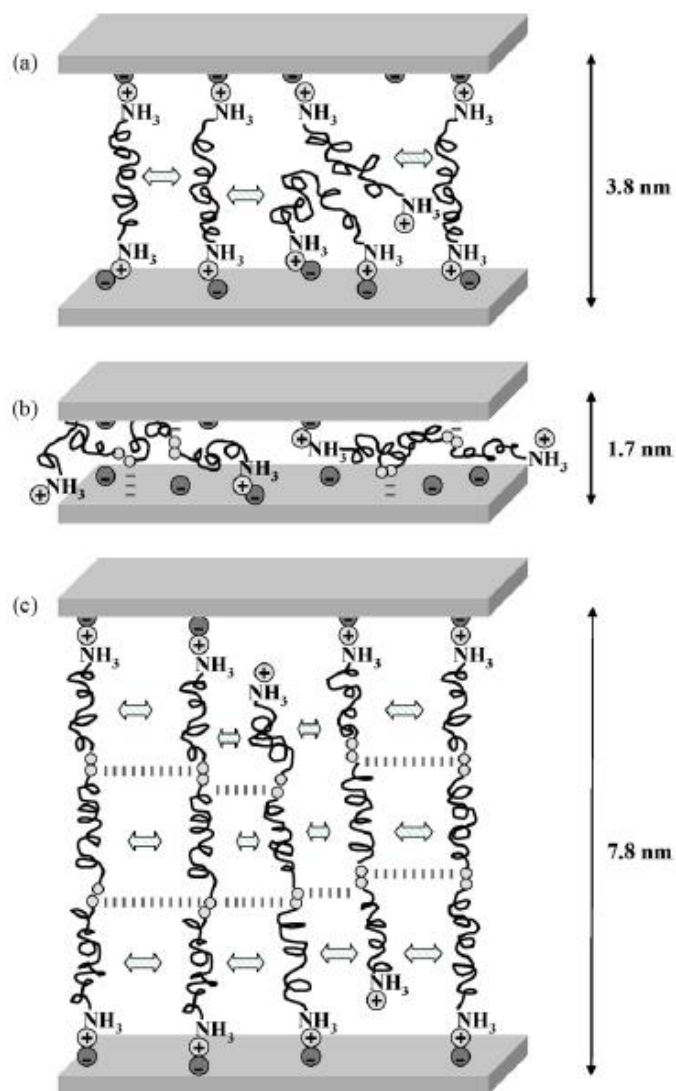
Figure. 6 Scheme of hydrogen bonding and hydrophobic effect in layered materials. (a)

POP2000 (b) POP400-AA (c) POP400-SA.

2.4 Electrochemical reaction

Before 1970s, batteries were irreversible.[24] Nowadays, we call those kinds of batteries

primary batteries. Two kinds of primary batteries were commonly used, one is

manganese battery, and the other is nickel battery. In a manganese battery, MnO_2 is

reduced to Mn_2O_3, in which a proton is inserted into MnO_2 to form $HMnO_2$. However,

HMnO$_2$ is unstable. It will easily release H$_2$O and give Mn$_2$O$_3$. Because the reduction of manganese battery eliminates water molecule in the post-intercalation stage, manganese batteries are irreversible battery. In 1973, Whittingham showed that the intercalation of Li to TiS$_2$ can produce a rechargeable battery.[24] This new rechargeable battery is based on the intercalation reaction shows as follow: Li $\rightleftharpoons$ Li$^+$ + e$^-$ and TiS$_2$ + Li$^+$ + e$^-$ $\rightleftharpoons$ LiTiS$_2$. As mentioned in the section of redox reaction mechanism, electrochemical intercalation is a process of reducing and oxidizing, with the procedure of lose and gain electrons to generate current. Figure 7[24] shows a simple scheme of lithium intercalation cell. The charging procedure is the reaction proceeds to the left side and to the right side to discharge. Three important parameters controlling electrochemical intercalation: First, the cell voltage is determined by free energy of reaction (E = ΔG/nF); Second, the stoichiometry of the intercalant control the cell capacity; Third, the power that a cell can deliver is determined by the intercalation reaction rate.

$$\oplus : \quad MX_n + yLi^+ + ye \rightleftharpoons Li_y\,MX_n$$

$$\ominus : \quad Li \rightleftharpoons Li^+ + e$$
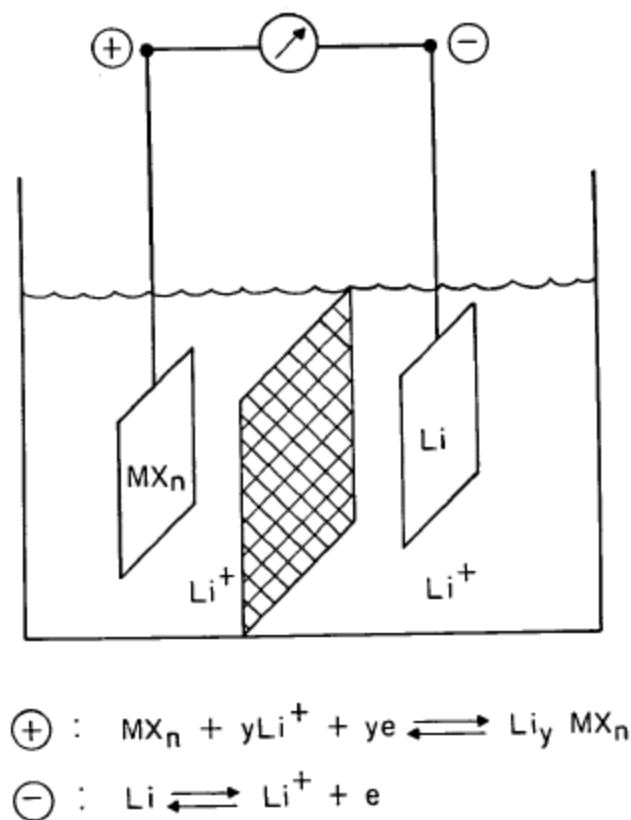
Figure 7. Scheme of simple rechargeable lithium battery.

Recently, scientists paid highly attention on the substitute electrode materials, electrochemical intercalant, or electrolyte to either increasing the battery capacity and lower the cost, or solve the environmental issues.[25,26] For example, Nuli et al. reported the electrochemical intercalation and deintercalation Mg^{2+} in magnesium manganese silicate by a high temperature solid-state reaction and sol-gel routes.[27,28] This result gives us another new idea that traditional univalent cations like Li^+ or H^+ can be substitute by divalent cation Mg^+.

3. Direct intercalation methods

The term "direct intercalation" refers to san approach in which layered material and intercalators directly react in a specific circumstance to achieve intercalation within one

step of reaction. Layered materials are typically solid, therefore intercalation reactions can proceed at the solid-gas, solid-liquid, and solid-solid interfaces, via different mechanisms discussed above.

3.1 Solid-gas intercalation

The modern intercalation research started from a paper in 1926 by Fredenhagen and coworkers, in which they reported the uptake of potassium vapor into graphite.[12] Since then, a wide range of graphite based intercalation compounds have been synthesized based on this solid-gas intercalation method.[29] In 1980s, Dresselhaust and coworkers summarized the work in this field and published a book to demonstrate the intercalation of graphite.[30] As described in that book, the two-zone vapor transport method is one of the most commonly used methods. As showed in Figure 8,[30] graphite and intercalant were separated in two individual tubes. The two tubes were heated at different temperature respectively. Graphite was heated at T_g ($T_{graphite}$) and intercalant was heated at T_i ($T_{intercalatant}$). The value of T_g-T_i corresponds well to the stage of the intercalation compound. The smaller of the value, the lower of the stage. Fig. 9[30] shows the classification of intercalation stage. Obviously, simply control the temperature difference between two reactants is not sufficient to gain an accurate control of the stage morphology. Recently, Zhao et al. reported by using this two-zone vapor transport method to intercalated few-layer graphite flakes with $FeCl_3$, and further determine the interlayer properties to solve the morphology problem.[31] The experiment apparatus is similar to the one used thirty years ago, as shows in Fig. 8.[30] Within today's technology, three layers and 2 layers of graphite were separated and further intercalate with $FeCl_3$

individually. By involving Raman spectra to determine the layer interaction between different stages to investigate the stage controlling factors.
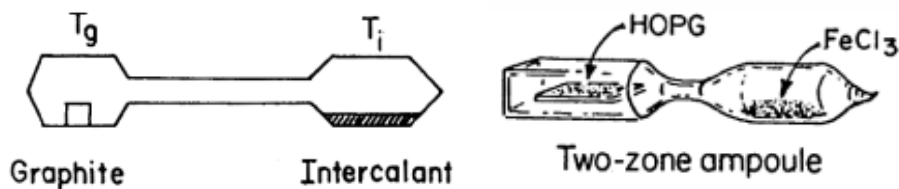
Figure. 8 left: two-zone vapor transport method scheme;[30] right: two-zone vapor transport apparatus.[30]
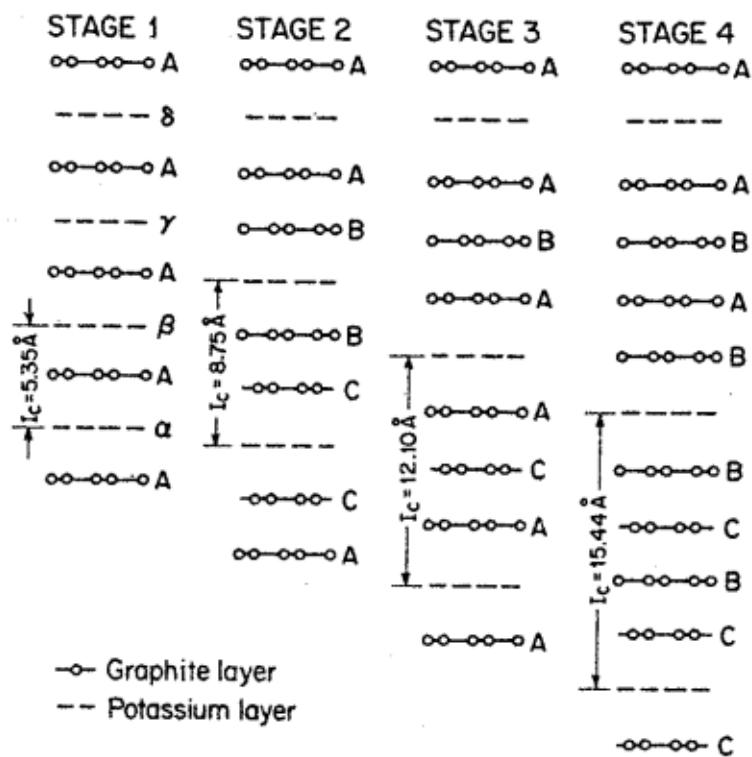
Figure. 9 Intercalation stage classification chart.[30]

The solid-gas intercalation method has been extended to many other layered compounds. And the apparatus was modified to incorporate various vacuum line techniques, allowing for treatments both before and after intercalation to promote the reaction. For example, Clearfield and coworkers[32] managed to intercalate alkylamines into layered copper phosphonates after initial removal of hydration water by vacuum and subsequent intercalation of copper phosphonates by various primary alkylamines, which occurred at solid-gas interface. The reaction apparatus used in this experiment is shown in Figure 10.[33] Copper phosphonate was placed in tube C, which was vacuum dried under heat with valve B closed, during which hydration water in copper phosphonate was removed. After that, valve A was close and valve B was open, the liquid amine in tube D was then evaporated under heating and reacted with pre-dehydrated copper phosphate in tube C to form intercalation compound.
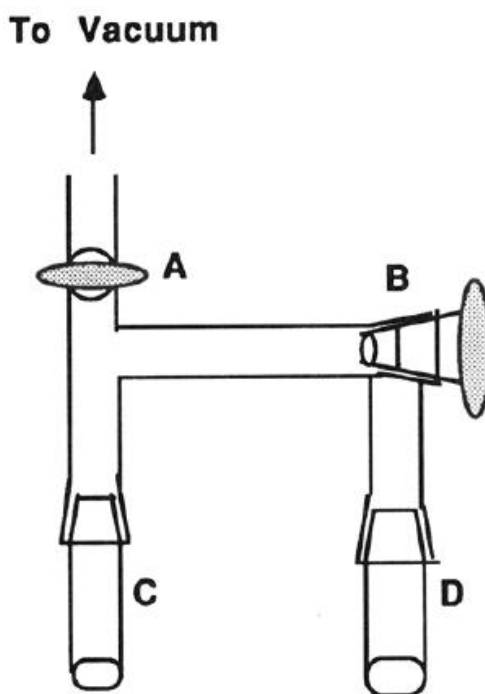
Figure 10. solid-gas reaction apparatus scheme.[33]

In the above experiment, the guest alkylamines can be vaporized to carry out the intercalation. In some other experiments, the guest materials are in solid or liquid state, but a carrier gas was introduced to "carry" the guest compound into layers. The carrier gas is only a transportation media. But considering the methodology is very similar to the solid-gas intercalation, it is also included in this section. For example, Cahen et al.[34] explored a method that used gaseous Al_2Cl_6 to form complexes with lanthanide chlorides, and then intercalate this gaseous lanthanide chlorides complex into the graphite layers. The process of reaction can be described in three steps: first, $AlCl_3$ was heated at 453 K to generate Al_2Cl_6 (3); second, $HoCl_3$ reacted with Al_2Cl_6 to form gaseous complex $HoAl_3Cl_{12}$ (4); third, $HoAl_3Cl_{12}$ complex react with graphite to form graphite intercalation compound (5).

$$2\ AlCl_3\ (g) \rightarrow Al_2Cl_6\ (g); \qquad (3)$$

$$(3/2)\ Al_2Cl_6\ (g) + HoCl_3(s) \rightarrow HoAl_3Cl_{12}\ (g); \qquad (4)$$

$$HoAl_3Cl_{12}\ (g) + nC \rightarrow nC\text{-}\ HoCl_3(s) + (3/2)\ Al_2Cl_6\ (g) \qquad (5)$$
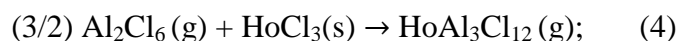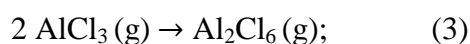
As we can see, in this series of equations, Al_2Cl_6 gas acts as a transport agent carrying the $HoCl_3$ into the graphite layers. Gas materials act as transportation agents are not very commonly to see in literatures to comparison with some liquid materials as a transportation agent such as water, alcohols, HCl or other sorts of liquid carriers. But to deal with some special compounds which are not able to or hard to dissolve in liquid, or even they can dissolve but still cannot achieve intercalation reaction, looking for a special gas transportation agent may give us another option to intercalate.

3.2 Solid-liquid intercalation

Solid-liquid intercalation is probably the most widely adopted method for intercalation. Solid layered hosts can be directly mixed with liquid intercatants to carrier out the intercalation. But more typically, layered hosts are dispersed in certain solvents, while guest species are dissolved in the same solvent, during which the liquid phase act as a reaction media for the intercalation reaction. The liquid media can help lower viscosity and expedite the reaction, and also improve reaction efficiency.

In a typical example, which was reported by Clearfield and coworkers,[35] α-ZrP was intercalated by hexylamine. α-ZrP was well pre-dispersed in acetone under one hour sonication firstly. Then, hexamine was added and directly mixed with α-ZrP-acetone dispersion to generate intercalation compounds.
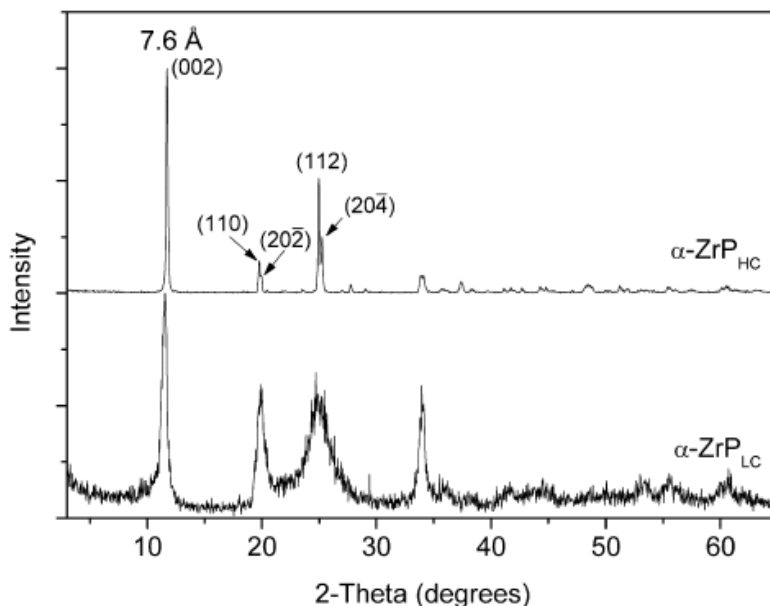
Figure. 11 XRD patterns of α-ZrP$_{HC}$ (4M-100°C-24h-RF)

and α-ZrP$_{LC}$ (3M-100°C-24h-RF).[35]
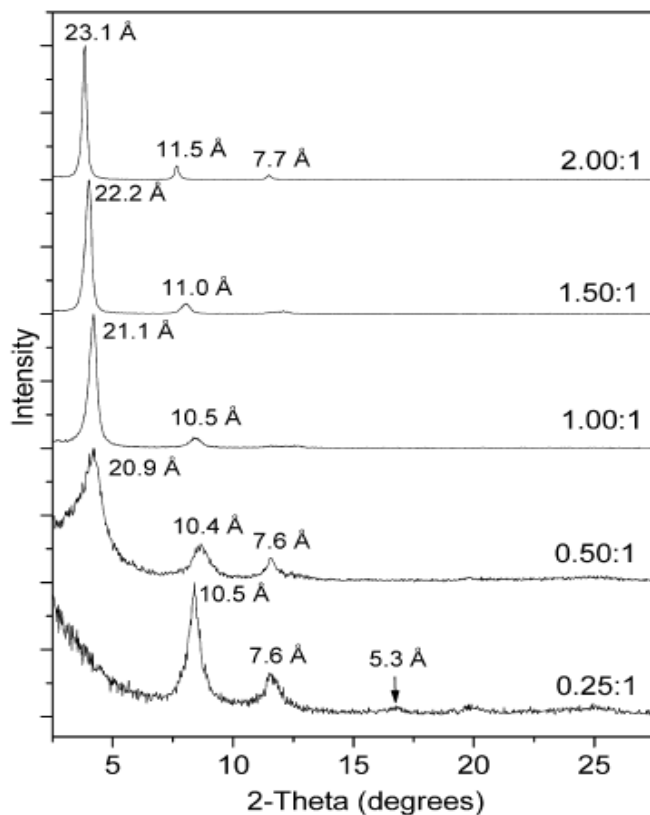
Figure 12. XRD patterns of α-ZrP intercalated by hexylamine at different intercalation ratios.[35]

The low crystallinity α-ZrP (α-ZrP$_{LC}$) was prepared by refluxing 3.0M phosphoric acid and zirconium oxychloride octahydrate for 24 hours under 100°C [α-ZrP$_{LC}$ (3M-100°C-24h-RF)]. Figure 11 shows that the layer distance of α-ZrP$_{LC}$ (3M-100°C-24h-RF) is 7.6Å. After intercalating hexylamine, α-ZrP galleries distance increased up to 23.1Å under the 2:1 intercalation molar ratio between hexylamine and α-ZrP (Figure 12). Figure 12 also indicates that with the increasing of intercalation ratio, the interlayer distance is increased. It is very similar with other kinds of linear alkylmonoamines intercalation compounds which have been well studied before[36,37,13]. In general, the increasing of

interlayer distance is due to the hexylamine chains increased incline angle with increasing the intercalating amount.

Another type of solid-liquid intercalation method was reported recently, in which external force (high pressure) was introduced to force liquid phase guest materials, such as water, water soluble molecules and ions, into the layered host.[38] To compare with the former example, this high pressure induced intercalation method does not involve chemical driving force. Instead, this method used pressure to "squeeze" soluble species into the graphite layered galleries. The scheme is showed in Figure 13.[38] In this method, the reaction time is relatively shorter compared to conventional reaction induced solid-liquid intercalation. Pressure serves an assistant role in the intercalation reaction, which offers an effective means to increase the intercalation rate. In addition, this approach is particularly valuable for those guest materials having little reaction with the host. The external pressure provides physical force to insert the guests into the galleries.
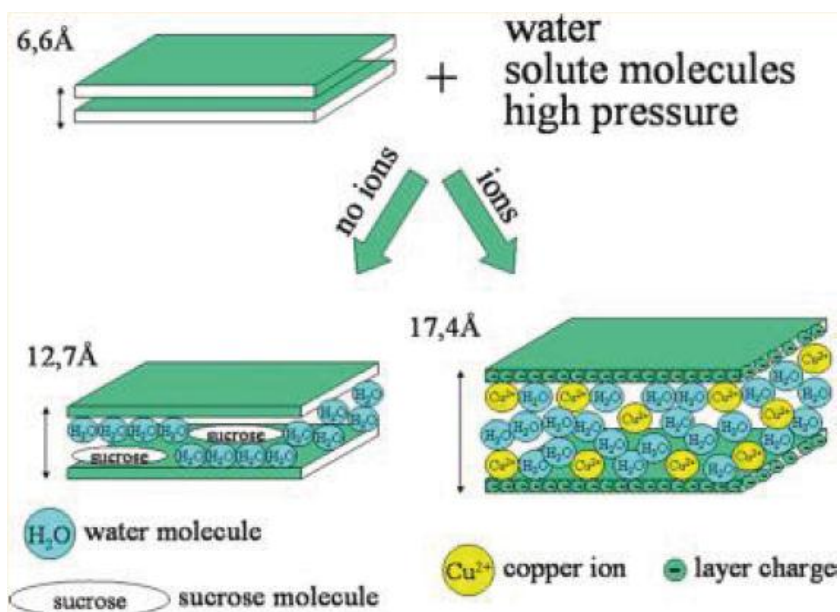
Figure 13. Scheme of pressure induced intercalation mechanism.[38]

3.3 Solid-solid intercalation

Solid-solid intercalation was initially developed to prepare intercalation compounds which are not accessible from solutions.[39] Unlike a conventional solution intercalation, this route can be proceeded under ambient or elevated temperatures via adsorption, a displacement or functional reaction, with main benefits of not requiring solvent, higher production yield, and short reaction time (as short as a few minutes).[39,40] The simplest means for solid-solid intercalation is manual grinding using a mortar and pestle, which can be easily scaled up via ball milling.[41,42,39] Solid-solid intercalation method has attracted high attention since it was invented, because it can be easily adopted in industry.

Milanesio et al. intercalated bioactive compound into $MgAl\text{-}NO_3$ LDH gallery via a solid-solid intercalation approach.[42] A commercial sunscreen product Eusolex (EUS), 2-phenylbenzimidazol-5-sulfonic acid, was used as guest compound. Initially, pre-formed $MgAl\text{-}NO_3$ was mechanically grinded and mixed with EUS. The mixture was mixed with 0.5 mL (concentration?) NaOH solution, which was subsequently manually ground in a mortar for one minute at room temperature, followed by drying at room temperature for one day. The resultant sample was designated as Sample 1. Sample 1 was washed 3 times using water and ethanol, and then was dried at room temperature for one day, to form Sample 2. The XRD characterization is shown in Figure 14.[42] The ion exchange reaction was evidenced by the presence of the peaks at 4.20° (*001*), 8.32° (*002*) and 12.38° (*003*), which is typical for a layered intercalation compound. Although there is a small amount of unreacted $LDH\text{-}NO_3$ remained in the final product, it is still a good way to achieve intercalation since the reaction time is very short.
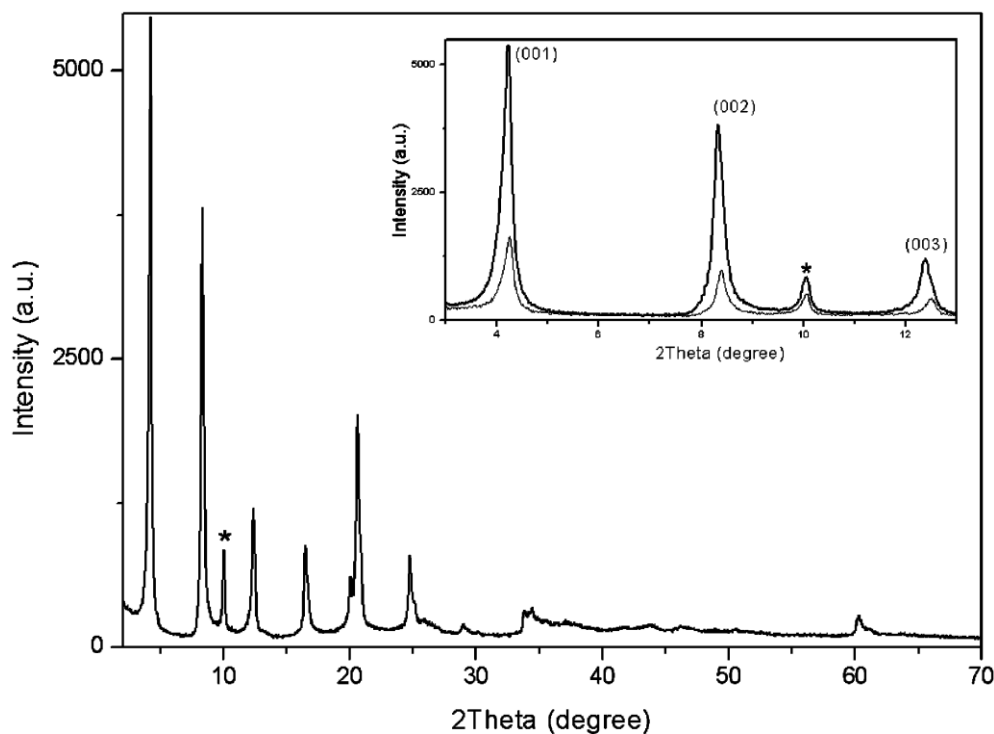
Figure. 14 XRD patterns for LDH-EUS intercalation compound (Sample 1). "*" refers to the unreacted LDH-NO$_3$. The inset shows the comparison of the peak intensity of Sample 1 (high intensity) and Sample 2 (low intensity).[42]

Hu, et al.[39] conducted a similar mechanochemical driven intercalation of α–zirconium phosphate (α-ZrP) by 1-butyl-3-methylimidazolium chloride (BMIMCl). Strictly speaking, BMIMCl melted when it was ground by a mortar and pestle, thus it is actually a solid-liquid intercalation. But because it follows virtually the same methodology as a typical solid-solid intercalation, it is discussed in this section. After α-ZrP was ground for three minutes in an agate motar to minimize small aggregates, BMIMCl was added and further ground for 10 min to generate the intercalation compound. The detail of formulation and appearance of α-ZrP/BMIMCl intercalation compounds is shown in Table 2. The XRD pattern (Figure 15) indicated that after mechanochemical intercalation,

the layer distance of α-ZrP clearly increased since BMIMCl was intercalated into the

gallery of α-ZrP layers.

Table 2. Formulation and appearance of α-ZrP/BMIMC intercalation

compounds.[39]

Sample	BMIM$^+$/exchangeable cation	BMIMCl weight percentage (wt%)	Product appearance
ZrP(3M-RF)-25	0.25:1	22.5	Powder
ZrP(3M-RF)-50	0.50:1	36.5	Powder
ZrP(3M-RF)-100	1.00:1	53.7	paste
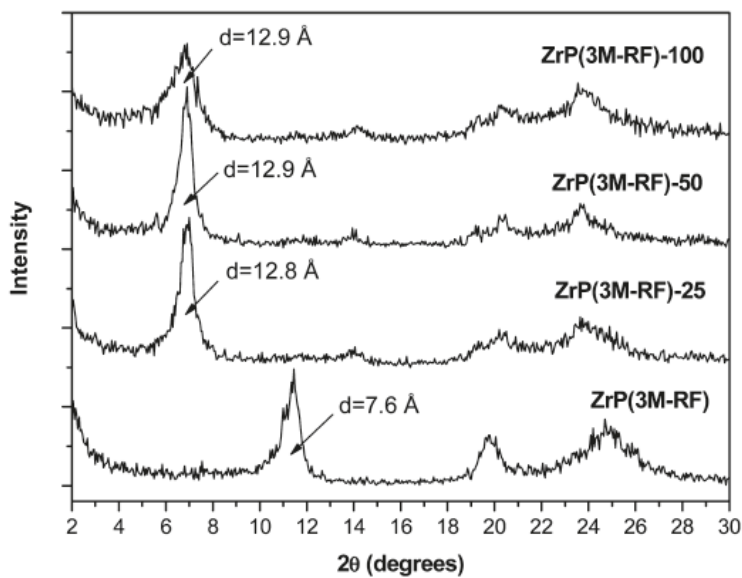
Figure 15. XRD patterns of ZrP(6M-HT)/BMIMCl intercalation compounds with

various BMIMCl loadings.[39]

Because the interlayer distance of α-ZrP is smaller than the dimension of BMIMCl, it is hard to directly intercalate BMIMCl into α-ZrP via conventional solid-liquid intercalation in a liquid media.[43] The mechanochemical process can provides external driving force to force $BMIM^+$ into the gallery to achieve intercalation. In addition to the above two example, many layered compounds have been intercalated by various guest species. For example, MMT was intercalated by various complexes and organic compounds,[40,44,45] α-ZrP was intercalated by solid amines,[46] and taeniolite was intercalated by amines.[47]. Overall, most solid-solid intercalations can be conducted within minutes. This great feature makes solid-solid intercalation promising for commercial applications.

4. Indirect intercalation methods

As the development of intercalation science, researchers wish to intercalate more and more functional guest species into the layered host to generate multifunctional intercalation compounds. However, these functional guest materials are usually too large to be directly intercalated via the one step intercalation approaches as discussed above. In order to address this issue, indirect intercalation was explored. Indirect intercalation refers to the multi-step intercalation reactions which are based on the pre-intercalation of layered compounds.[48] The idea is to use small molecules to intercalate into layered materials first, which helps to pillar the layers to a large interlayer distance to facilitate the intercalation of large guest species at the second step. Due to the nature of multistep intercalation, such intercalations typically follow the ion-exchange mechanism.

For example, the interlayer distance of α-ZrP is ca. 7.6 Å, while the maximum opening size between α-ZrP layers is only ca. 2.6Å.[49] Therefore, only the guests of less

than 2.6 Å can be directly intercalated into the cavities.[50] Intercalating larger sized guest

materials need to pre-intercalate the layers with selected guests to expand the interlayer

distance.[50] Vliers, et al. pre-intercalated α-ZrP with hexylamine via liquid-liquid

intercalation method discussed above to increase the interlayer distance from 7.6 to xxx

Å.[48] $Ru(bpy)_3^{2+}$ cations were subsequently intercalated into the hexylamine-

preintercalated α-ZrP.[48] Similarly, Bermúdez et al. pre-intercalated α-ZrP with

butylammonium cations to enhance the interlayer distance from 7.6 to xxx Å. The pre-

intercalation compound was then intercalated by luminescent probe 1-

pyrenemethylamine (PYMA) for functional applications. While the pre-intercalation to

pillar the layered compounds does facilitate the following intercalation process, the

introduction of pre-intercalants may generate issues, particularly for catalytic and

biomedical applications. To address this problem, Martí and Colón[51] refined the strategy

to insert water molecules, instead of regular chemicals, into the galleries to increase the

interlayer distance. Furthermore, rather than intercalating water molecules into the pre-

synthesized layered compounds, they managed to directly synthesize a layered

compounds containing a high concentration of hydration water, $Zr(HPO_4)_2 \cdot 6H_2O$ (θ-ZrP),

to replace the conventional $Zr(HPO_4)_2 \cdot H_2O$ (α-ZrP). Clearfield et al.[52] first observed this

θ phase zirconium phosphate and characterized the interlayered distance to be 10.3 Å[53].

(Figure 16.)
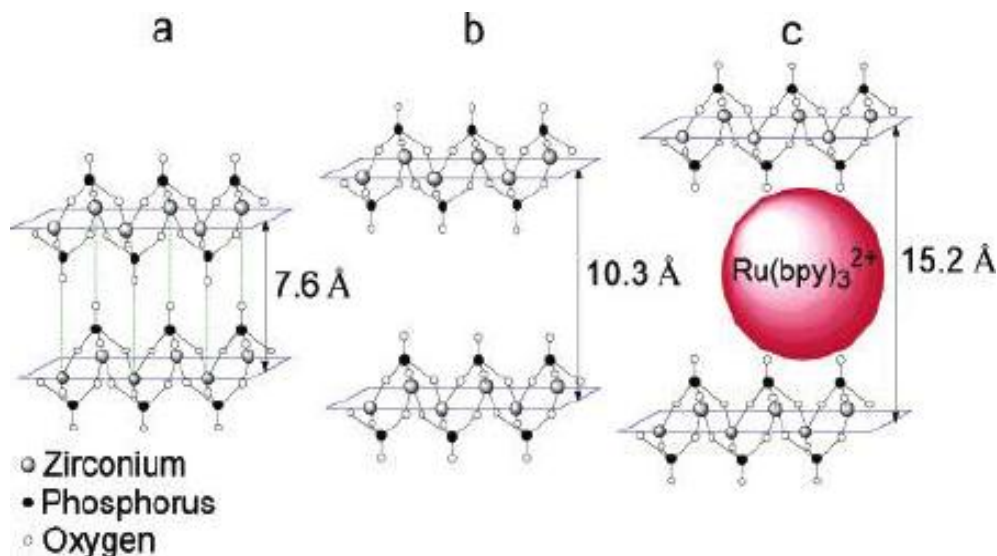
Figure 16. Idealized representation of three different zirconium phosphate phases: (a) α-ZrP, (b) θ-ZrP, (c) Ru(bpy)$_3^{2+}$ exchanged ZrP. Hydrogen atoms and water molecules are not shown for clarity.[51]

θ-ZrP can be synthesized by constant stirring ZrOCl$_2$•8H$_2$O with 6M H$_3$PO$_4$ solution under 94°C for 48 hours.[54] the increased interlayer distance from 7.6 to 10.3 Å offers a much larger flexibility to accommodate large guest species. For example, Ru(bpy)$_3^{2+}$ can be directly intercalated into θ-ZrP by simply mixing θ-ZrP and Ru(bpy)$_3^{2+}$ in an aqueous solution under constant stirring at ambient temperature for 4 days.[51] Figure 17 shows that after ion exchanging of Ru(bpy)$_3^{2+}$, the interlayer distance of θ-ZrP increased up to 15.2Å. With the increasing of Ru(bpy)$_3^{2+}$ loading level, the luminescence intensity of Ru(bpy)$_3^{2+}$/ZrP intercalation compounds also increased.
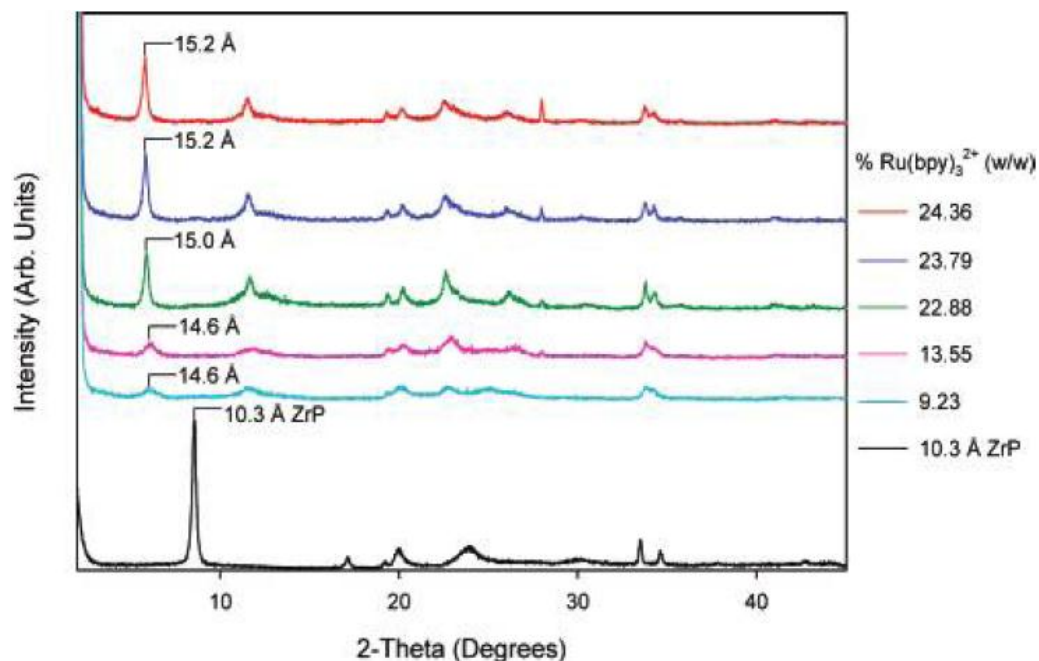
Figure 17. XRD patterns for Ru(bpy)$_3^{2+}$ exchanged ZrP materials at various loading levels (% w/w) and 10.3Å ZrP.[51]

By using directly synthesized θ-ZrP instead of amines pre-intercalate α-ZrP, it not only shortens the procedures for achieving intercalation, but also eliminated the negative effect from amines, which significantly affects the luminescent properties of Ru(bpy)$_3^{2+}$.[48,55] As a result, this kind of pre-intercalation methods were widely used recently in the intercalation of other luminescent metal complexes,[56,57,58] protein,[59] ionic liquids,[43] ferrocenium,[60] et al.

5. Factors influencing the intercalation process

The interlayer distance is by far the most critical reason that influences the intercalation process and results, which has been discussed in various examples above. In addition to that, several other factors also play important roles in intercalation. By controlling these factors, more ideal intercalation compounds can be synthesized.

5.1 Regularity of interlayer space

The influence of interlayer regularity of the layered hosts is widely known in intercalation science. In general, the layered hosts with a low crystallinity typically possess layer distortions or defects. These distortions/defects are probably not ideal for certain applications, but are actually beneficial for intercalation. Sun et al. explored the influence of layered host crystallinity on the intercalation process.[61] By controlling the synthesis conditions, α-ZrP hosts with two distinctive levels of crystallinity were prepared The α-ZrP host with lower crystallinity exhibited poorer interspace regularity due to the existence of layer defects, as evidenced by XRD characterizations. When the two α-ZrP hosts were intercalated by a polyoxyalkyleneamine (Jeffamine M715) at various intercalation ratios, they exhibited very different trends. Figure 18 shows XRD patterns of the intercalation products after intercalated by M715 at different molar ratios. The α-ZrP with low crystallinity can be easily intercalated at a low intercalation ratio, and the intercalation progressed quickly. The intercalant M715 can be inserted into the galleries of α-ZrP and uniformed spread with the assistance of ultrasonication. However, the α-ZrP with high crystallinity is much more difficult to be intercalated at the low intercalation ratios. A complete intercalation was not achieved until more M715 was available. This suggested that the diffusion introduced by ultrasonication is not sufficient the overcome the energy barrier, only the energy provided by the reaction between α-ZrP and the host can overcome the energy barrier to achieve intercalation. The reason that the host with a low crystallinity can be more facilely intercalated is because of the presence of defects and distortions on layers, which offers. more chances for the guest species to penetrate in.
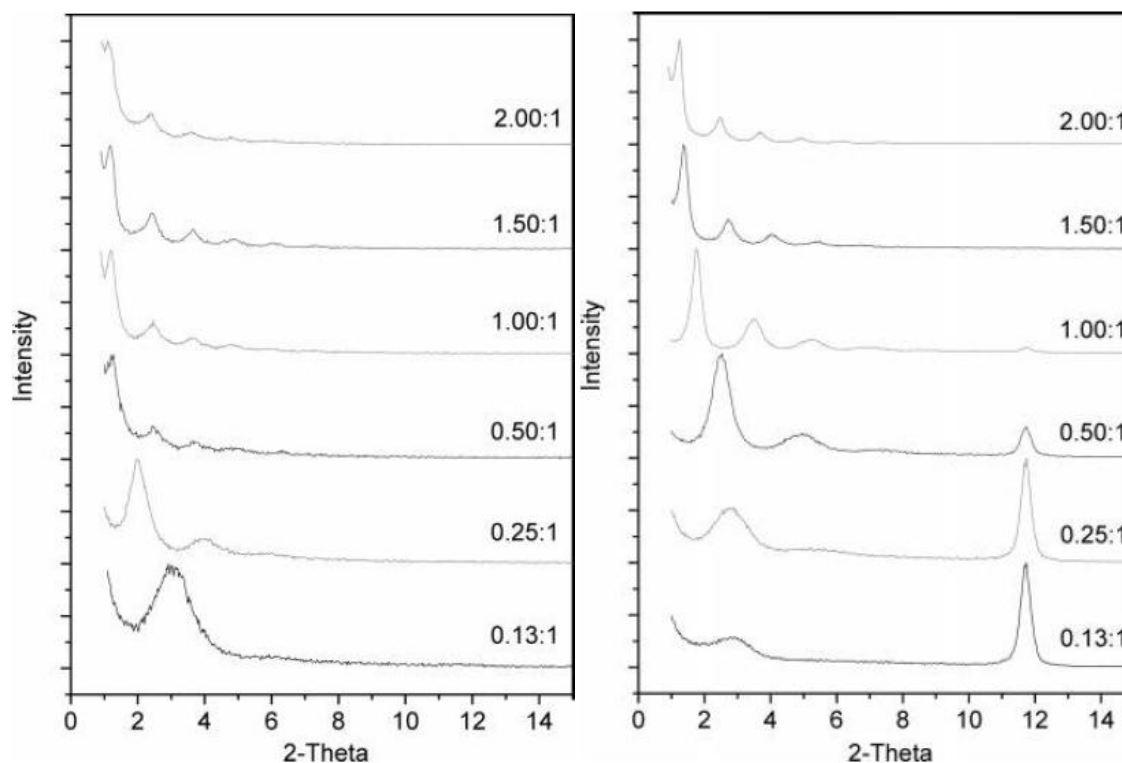
Figure 18. XRD patterns. Left: ZrP/Jaffamine (3M) in different molar ratio; right: ZrP/ Jaffamine (6M) in different molar ratio.[61]

5.2 Interlayer space

Interlayer space is another key factor for intercalation reactions. It has been widely accepted and proved that enhancing interlayer distance by pillaring the layers will help the following intercalation process, and that is how the indirect intercalation approach developed as discussed above. However, how the interlayer space is packed has been largely ignored. Boo et al. designed an experiment to pre-intercalate layered α-ZrP by a mixture of bulky cyclohexylamine and long chain dodecylamine to intentionally introduce voids between pre-intercalated α-ZrP layers. They found that although the interlayer distance of the compound pre-intercalated by a mixture of cyclohexylamine and dodecylamine (28 Å) is lower than the one intercalated by pure dodecylamine (36 Å),

because cyclohexylamine has a lower dimension, the former one was actually a much better host for subsequent intercalation because of the formation of porous pathways. (Figure 19.) The scheme shows in Figure 20. This experiment clearly indicates that the interlayer distance is not the only limitation for large guest molecules, the voids between the layers will also facilitate the insertion of guest species.
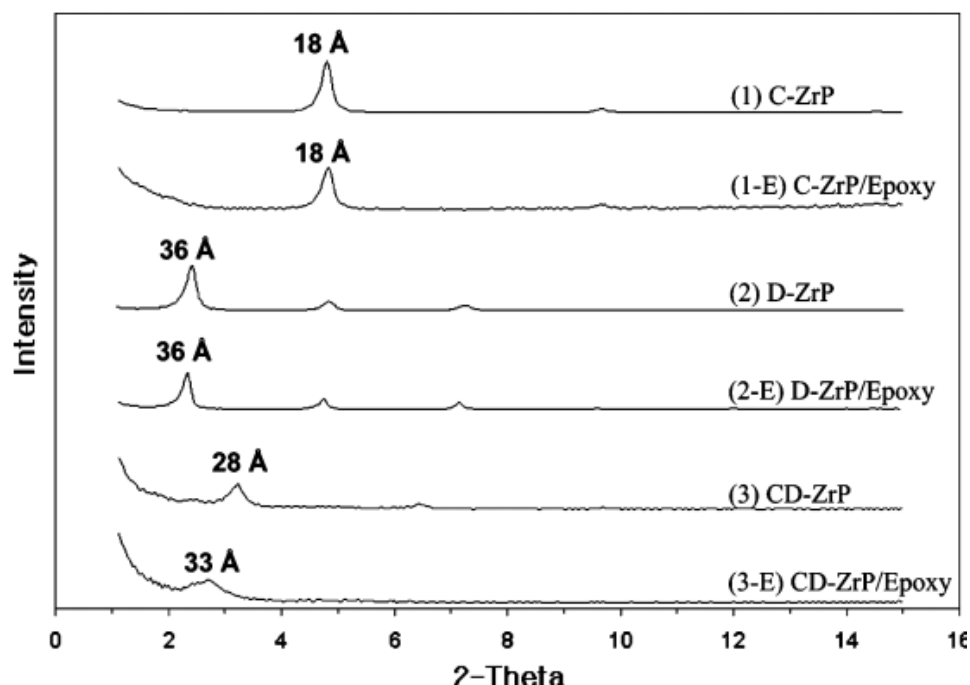
Figure 19. XRD patterns of intercalated ZrP with cyclohexylamine (C-ZrP), dodecylamine (D-ZrP), and a mixture of the two (CDZrP), with each followed by the mixing with epoxy monomer.[62]
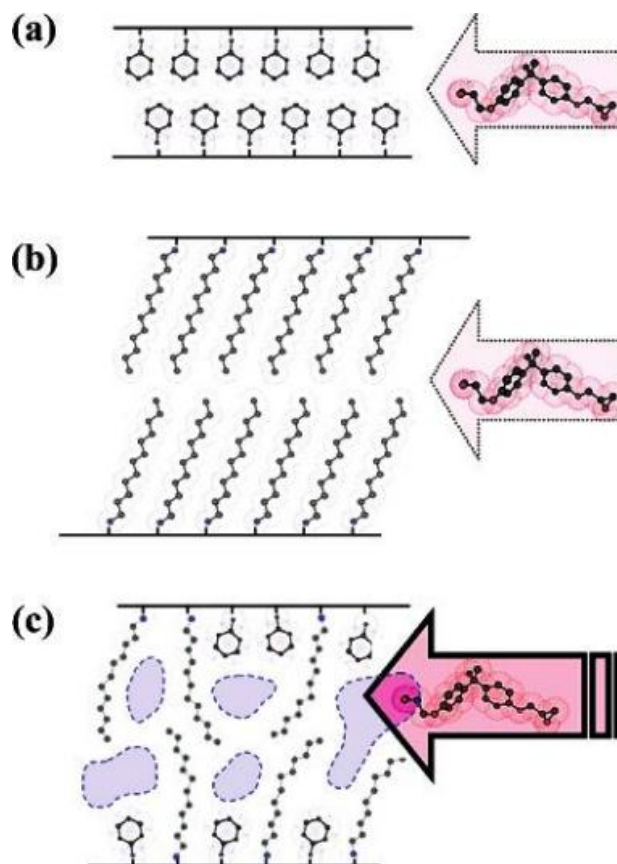
Figure 20. Schematic illustrations of interlayer spacing of α-ZrP treated with different organic modifiers: (a) cyclohexylamine, (b) dodecylamine, and (c) an equal mixture of cyclohexylamine and dodecylamine.[62]

5.3 Summary

In this section, factors that can influence intercalation were discussed. These factors can be used as enhancement but sometimes they are act as limitations. Such as if we want to synthesis high crystallinity host materials and also want to gain better intercalation ratio, we need to increase the amount of guest materials or increase reaction temperature or time. Because of the limitations discussed above, new approaches have been developed to achieve intercalation, such as exfoliation and reassembly method and layer-by-layer intercalation method, will be discussed below.

6. Achieving intercalation structure via pre-exfoliation

Pre-exfoliation of layered compound can be considered as an extreme of pre-intercalation discussed above. Strictly speaking, the morphology formed via exfoliation and re-assembly is different from the conventional intercalation procedures. However, overall it also leads to a layered structure composed of layered inorganic host and guest species alternating structure, mimicking regular intercalation compounds, and thus it is also discussed here. One advantage of exfoliation and reassembly lies in the fact that this method can produce thin films with a large dimension and thus beneficial for some industrial applications.

6.1 Exfoliation and reassembly

"Exfoliation and reassembly" refers to a method to pre-exfoliate layered materials into individual nanosheets, which are subsequently reassembled with guest species to form a layered structure.[63,64,65]

The exfoliation and reassembly approach was first reported by Kumar and coworkers[63] when they tried to intercalating proteins into α-ZrP. The protein molecules are too large to be directly intercalated into α-ZrP. They managed to first exfoliate layered α-ZrP into individual nanosheets, then mixing the nanosheets with protein molecules. After re-assembling the mixture followed by freeze drying, proteins were immobilized between α-ZrP sheets. The details of proteins were listed in Table 3, and the XRD patterns were showed in Figure 21, which indicates that by using the "exfoliation and reassembly" method, proteins were intercalated into the gallery of α-ZrP.

Table 3. Interlayer spacings, stoichiometried and binding constants observed for

immobilized α-ZrP/proteins composites.[63]

α-ZrP/proteins	Stoichiometry (μM)	K_b/M^{-1}	d spacing (Å)	Protein size (Å)
No protein	-	-	7.6	-
TBA	-	-	18.6	-
Myoglobin	12	2×10^5	54	$30\times40\times40$
Lysozyme	40	1.33×10^6	47	$32\times32\times55$
Hemoglobin	14	5.4×10^6	66	$53\times54\times65$
Chymotrypsin	3	2.5×10^5	62	$40\times43\times65$
Glucose oxidase	1.1	5.6×10^4	116	$43\times51\times68$
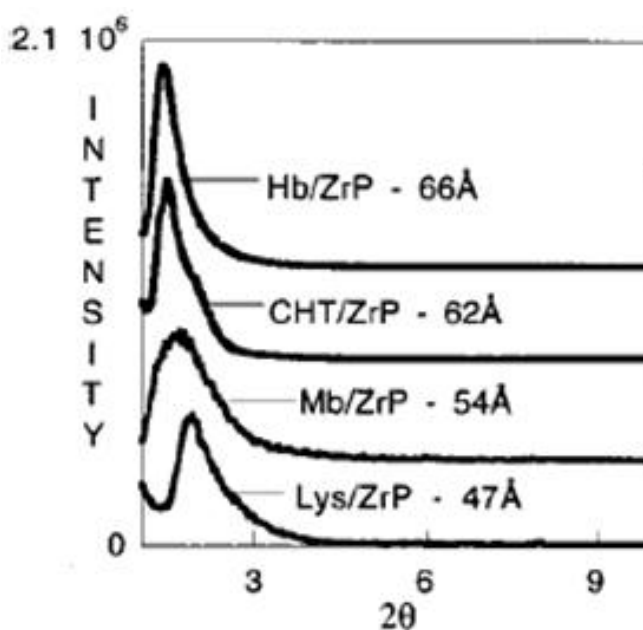
Figure 21. XRPD patterns of protein/α-ZrP composite materials.[63]

Similarly, Coronado et al. explored to intercalate two-dimensional oxalate-bridged coordination polymer $[Mn^{II}Cr^{III}(ox)_3]^-$ ($ox=C_2O_4^{2-}$) into layered double hydroxides (LDH) layers.[66] The experiment procedures are demonstrated in Figure 22.[66] The pre-formed ZnAl-CO$_3$ LDHs (1) were initially exchanged by a mixture of HNO$_3$/NaNO3 to form ZnAl-NO$_3$ (2). Second, finely ground ZnAl-NO$_3$ powder samples were dispersed in formamide, further stirred and ultrasonicated to fully exfoliate LDH. Due to the positive charge on the exfoliated LDH sheets surface, when negative containing coordination polymer $[Mn^{II}Cr^{III}(ox)_3]^-$ was added into the solution, ZnAl-$[Mn^{II}Cr^{III}(ox)_3]$ (3) intercalation compound was produced rapidly.
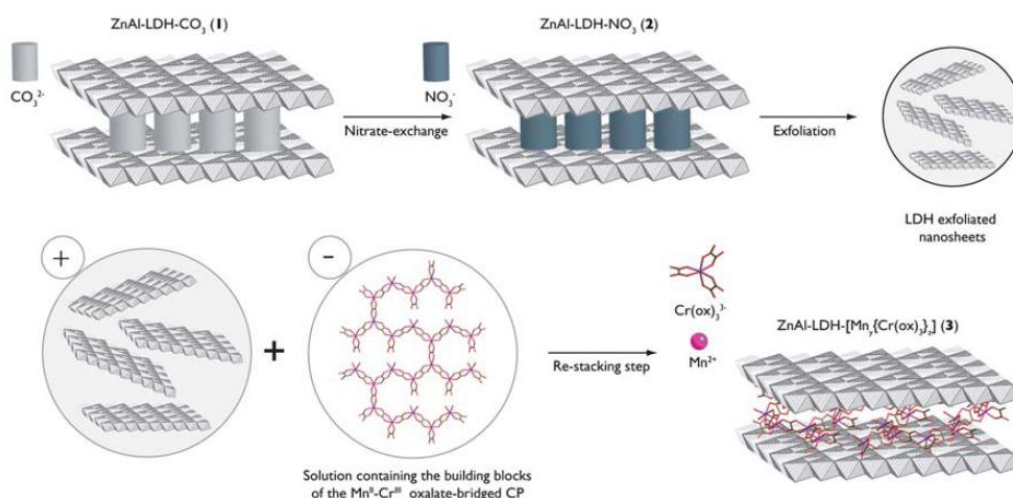
Figure 22. Scheme of exfoliation and reassembling.[66]
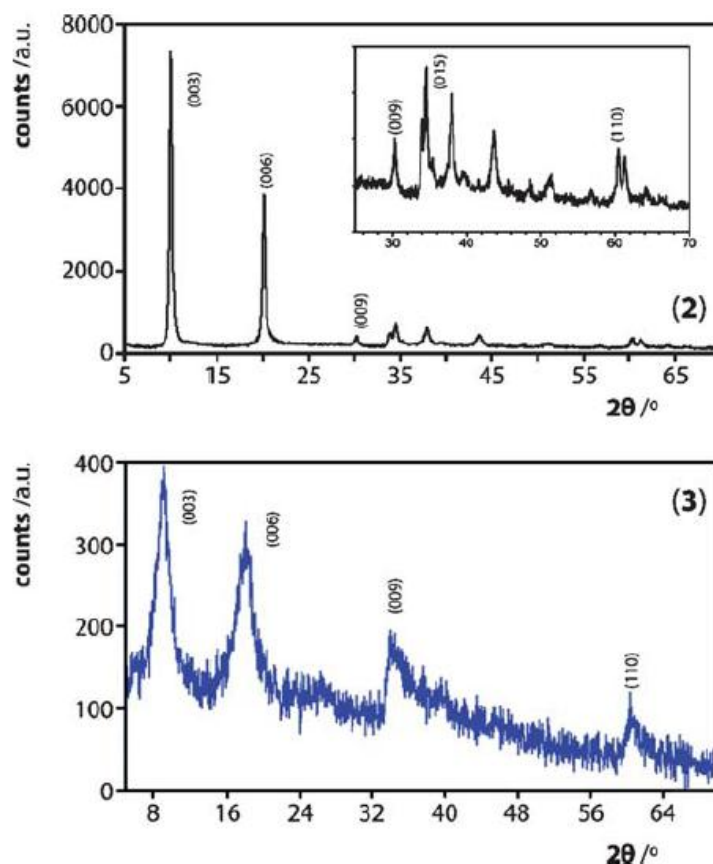
Figure 23. XRD patterns of: ZnAl-NO$_3$ (2) and ZnAl-[Mn^{II}Cr^{III}(ox)$_3$] (3).[66]

Figure 23 shows the typical LDH XRD patterns of samples (2) and (3).[66] The main difference between (2) and (3) is the layer distance. The basal spacing of (2) is 8.90Å which is in good agreement with reported LDH compounds, while the interlayer distance of sample (3) is 9.69 Å. The layer distance expansion is due to the intercalation of [Mn^{II}Cr^{III}(ox)$_3$]$^-$ guests.

Exfoliation-reassembly method is usually applied in the intercalation of large guest species, such as proteins and enzymes,[67] and polymers.[65] The layered materials can act as a protector to shield proteins and polymer to minimize decomposition or lose activities.[68]

6.2 Layer-by-Layer self-assembly

Layer-by-layer (LbL) can be considered as a special exfoliation-reassembly approach, which generates intercalated structure via alternating physisorption of charged exfoliated nanosheets and an oppositely charged polyelectrolytes.[69] LbL can lead to the formation of large size thin films, coatings, etc. with intercalated structure. But meanwhile, LbL is demanding on the components that can be potentially assembled. For example, small molecules and neutral components typically cannot be incorporated within the layers. A typical process of LbL self-assembly is shown in Figure 24.[69]
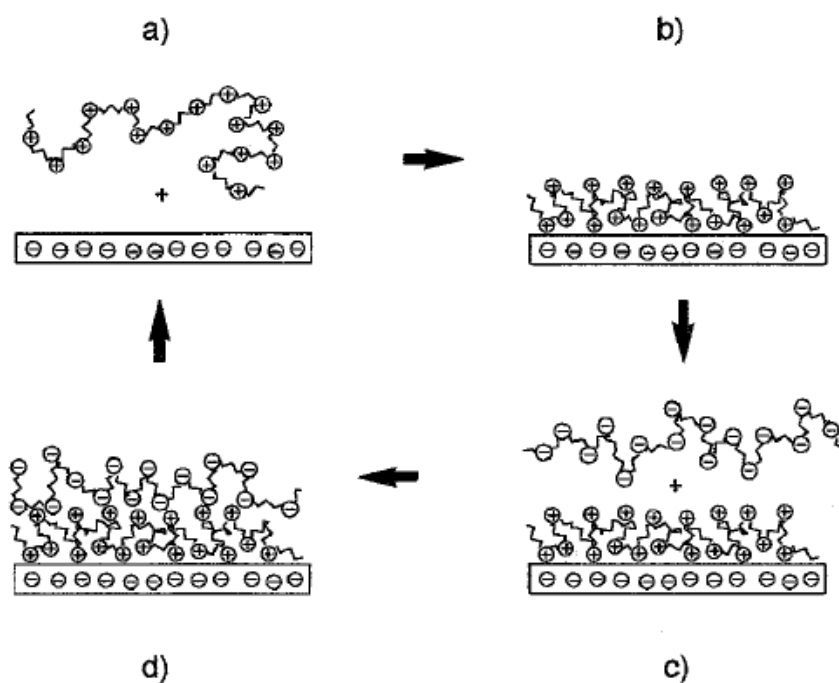
Figure 24. Scheme of layer-by-layer procedure.[69]

Patro et al. recently reported to make poly(vinyl alcohol) (PVA)-laponite clay multilayered composite via LbL method.[70] PVA was pre-dissolved in 80°C water to make PVA 1% solution. Laponite clays were also pre-dispersed into water under magnetic stirring. A control sample was named P-20 pphpl (parts per hundred polymers) which is

made by 100 mg of PVA plus 20 mg of laponite. The procedure of layer-by-layer coating underwent following steps: (1) immersion into PVA solution for 1 minute; (2) immersion into water for 2 minute; (3) immersion into laponite solution for 1 minute; (4) immersion into water for 2 minute followed by procedure (1). The aim of dipping the film into water after either immersed into PVA or laponite is to wash out the excessive molecules stick on the film to make sure every single layer is monolayer. After estimated numbers of layers have already formed, multilayers film rinsed by large amount of water and then dried.
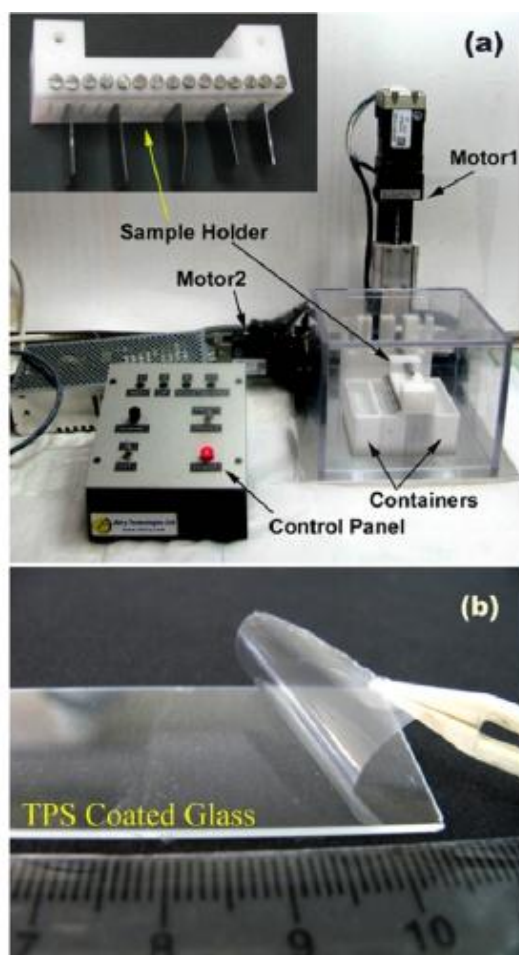
Figure 25. (a) homemade layer-by-layer set-up; (b) peeling off a 100-bilayer film (~5μm thickness).[70]

The homemade layer-by-layer set-up is programmable (Figure 25.). The holder immerses the sample substrate into different solvent container step by step followed by former procedures.
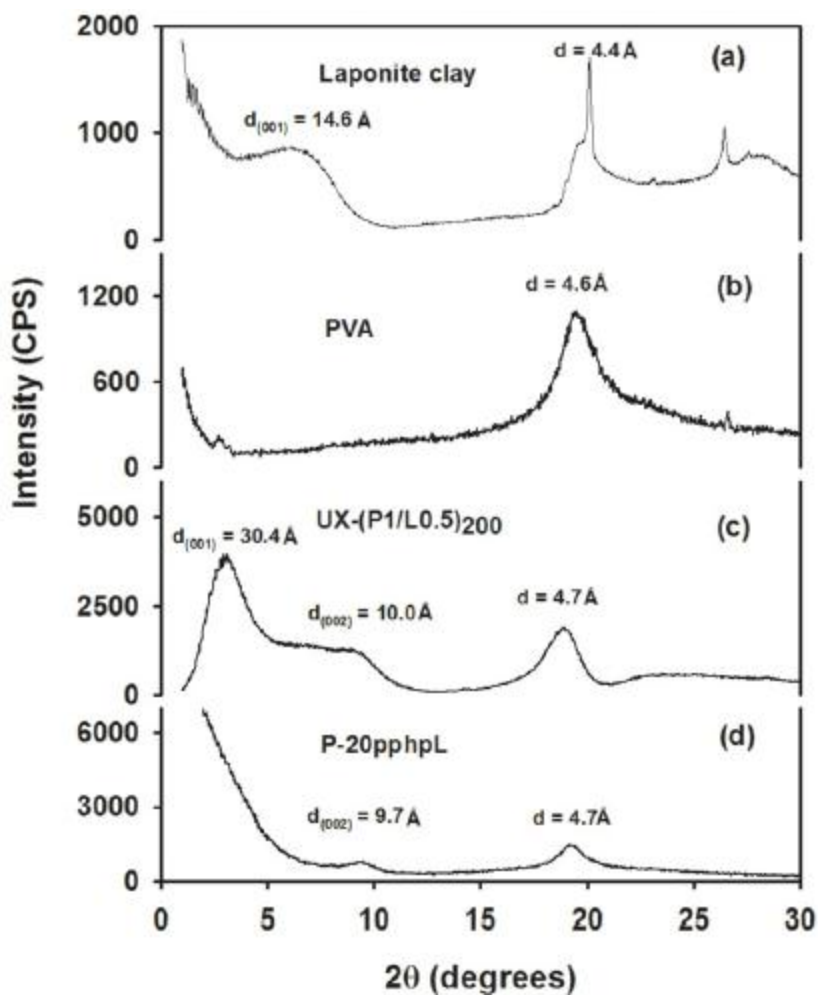
Figure 26. XRD patterns (a) pure laponite clay; (b) pure PVA; (c) 200-bilayer LbL film; (d) P-20 pphpl.[70]

In comparison to the layer distance of pure laponite (Figure 26 a) with the 200-bilayer layer-by-layer film, it is obvious that the layer distance increased form original 14.6Å to 30.4Å, which indicates that with the layer-by-layer intercalation, the thickness of individual layers increased via exist of polymer between layers. The absence of the (001)

peak of P-20 pphpl shows that the laponite clay lost the layered structure. The scanning electron microscope (SEM) image of the fractured cross-section shows the multi-layers arrayed ordered and the thickness of cross-section is very thin, just about 7 μm (Figure 27.).[70]
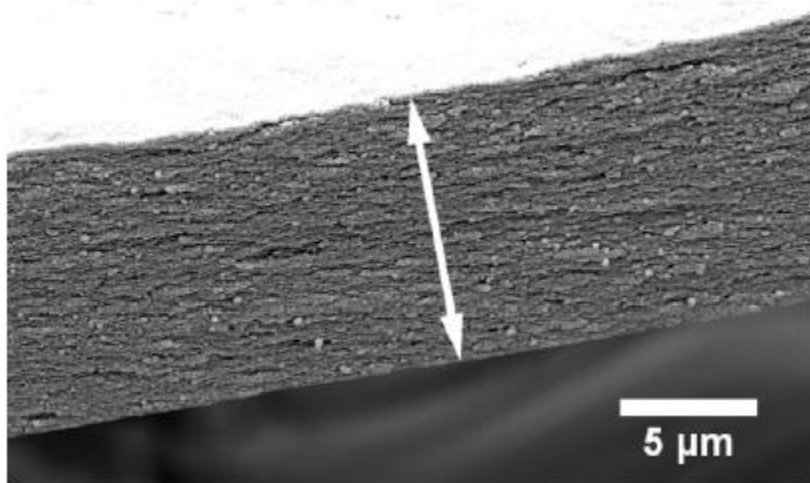
Figure 27. SEM image of 200-layer film cross-section[70]

With the development of LbL self-assembly, it is certain that more materials will be adopted to prepare layered hybrids with an intercalated structure.

7. Applications

In the past few decades, the intercalation materials have also been well developed due to their extraordinary importance and wide applications. It is expected that the applications of intercalation compound will be much wider in the near future. Herein, rather than giving a comprehensive review of the wide applications of intercalation compounds, we would instead highlight some key applications of intercalation compounds.

7.1 Catalysis

Layered intercalation compounds have found wide applications in catalysis. The solid inorganic layers can not only protect the intercalants from damaging by either high temperature or other extreme crucial reaction circumstances to improve the catalysis efficiency, but also may lead to heterogeneous catalysts for facile separation after reaction.[71,72,73,74,75] Hu et al. reported to immobilize ionic liquid BMIMCl into the layered α-ZrP via a mechanochemical approach, converting conventional BMIMCl into a supported heterogeneous catalyst, which maintained activity during CO2 coupling reaction, meanwhile can be easily recycled and re-sued.[39] Some of the catalysts were first intercalated into layered materials, and then exfoliate the layer sheets to promote their catalytic capacity.[71]

Layered intercalation compounds are also applied in biological catalysis field. By immobilizing enzymes into the layered materials, the enzymes will possess a higher stability, which is beneficial for certain catalysis applications.[63]

7.2 Medical applications

Medical and pharmaceutical applications of intercalation compounds have been well developed. Since the inorganic layers can confine drug molecules in their interspace, drugs such as insulin or enzymes can be protected and gradually released.[59] The enzymes that are confined within the layers can be used in medical field to treat some enzyme lacking diseases.[63]

While a number of medical and pharmaceutical applications have been reported, the challenges still remain and are to be fully addressed due to the following reasons: (1) the layered hosts must be nontoxic and edible; (2) typically, the protein or drug molecules are

too large to be direct intercalated,[63] meanwhile pre-intercalants, which might generate negative impact to either the drugs or body, are highly undesirable. Thus more detailed investigations are necessary for further development in this field.

7.3 Energy related applications

Battery represents one of the most typical and traditional applications of layered intercalation compounds. As introduced in the electrochemical intercalation section, battery evolved from ir-rechargeable to rechargeable. Layered intercalation compounds have also been applied in solar cells.[16] With the protection of layered materials, the solvent leakage issues can be partially solved.[16] In the future, substitution of expensive electrode materials will be critical. The exploration to use inexpensive Mg^{2+} or Fe^{2+} cations to substitute Li^+ has been reported.[26] However, critical issues still exist, such as low electron capacity, and unstable low voltage. More investigations will be focused on these issues in the future.[26]

8. Summary

In order to generate unique layered intercalation compounds, novel intercalation methods are to be further developed. It is believed that with the development of new intercalation methodology, layered intercalation compounds will be more and more widely used in our daily life.

References

1.	(a) Müller-Warmuth, W.; Schöllhorn, R., *Progress in Intercalation Research*. Kluwer Academic Publisher: Dordrecht, The Netherlands, 1994; (b) O'Hare, D., Inorganic intercalation compounds. In *Inorganic Materials*, Bruce, D. W.; O'Hare, D., Eds. John Wiley & Sons: West Sussex, 1992; pp 165-235.

2.	Mitzi, D. B., Thin-Film Deposition of Organicâˆ'Inorganic Hybrid Materials. *Chemistry of Materials* **2001,** *13* (10), 3283-3298.

3.	Schöhorn, R., Intercalation Systems as Nanostructured Functional Materials. *Chemistry of Materials* **1996,** *8* (8), 1747-1757.

4.	Kurosumi, S.; Nagamura, N.; Toyoda, S.; Horiba, K.; Kumigashira, H.; Oshima, M.; Nishimura, S.-i.; Furutsuki, S.; Yamada, A.; Mizuno, N., Resonant Photoemission Spectroscopy of the Cathode Material LixFePO4 for Lithium-Ion Battery. *The Journal of Physical Chemistry C* **2011**.

5.	Kreuer, K.-D., Proton Conductivity: Materials and Applications. *Chemistry of Materials* **1996,** *8* (3), 610-641.

6.	(a) Aizenberg, J.; Hanson, J.; Koetzle, T. F.; Weiner, S.; Addadi, L., Control of Macromolecule Distribution within Synthetic and Biogenic Single Calcite Crystals. *Journal of the American Chemical Society* **1997,** *119* (5), 881-886; (b) Albeck, S.; Aizenberg, J.; Addadi, L.; Weiner, S., Interactions of various skeletal

intracrystallinecomponents with calcite crystals. *Journal of the American Chemical Society* **1993,** *115* (25), 11691-11697.7. Mehnert, C. P., Supported Ionic Liquid Catalysis. *Chemistry – A European Journal* **2005,** *11* (1), 50-56.

8. Alberti, G.; Costantino, U.; Szirtes, L., Effect of ionising radiation on intercalation compounds and organic derivatives of zirconium phosphates I. Effect of irradiation on carboxyethylphosphonic and phenylphosphonic acids and on the corresponding layered zirconium phosphonates. *Radiation Physics and Chemistry* **1997,** *50* (4), 369-376.

9. Mellor, J. W., The beginning of porcelain in China. *Nature (London, U. K.)* **1917,** *100* (Copyright (C) 2012 American Chemical Society (ACS). All Rights Reserved.), 88-9.

10. Weiss, A.; Weiss, A., Intracrystalline swelling of dititanates. *Angew. Chem.* **1960,** *72* (Copyright (C) 2012 American Chemical Society (ACS). All Rights Reserved.), 413-15.

11. Bruce, D. W.; O'Hare, D.; Editors, *Inorganic Materials*. Wiley: 1992; p 543 pp.

12. Fredenhagen, K.; Cadenbach, G., Combination of potassium with carbon. *Z. Anorg. Allg. Chem.* **1926,** *158*, 249-63.

13. Clearfield, A.; Costantino, U., Layered metal phosphates and their intercalation chemistry. In *Comprehensive Supramolecular Chemistry*, Alberti, G.; Bein, T., Eds. Elsevier: Oxford, UK, 1996; Vol. 7, pp 107-149.

14. Clearfield, A., *Inorganic Ion Exchange Materials*. CRC Press: Boca Raton, FL., 1982; p 1-74.

15.	Wang, Q.; O'Hare, D., Recent Advances in the Synthesis and Application of Layered Double Hydroxide (LDH) Nanosheets. *Chemical Reviews* **2012,** *112* (7), 4124-4155.

16.	Bastianini, M.; Costenaro, D.; Bisio, C.; Marchese, L.; Costantino, U.; Vivani, R.; Nocchetti, M., On the Intercalation of the Iodine–Iodide Couple on Layered Double Hydroxides with Different Particle Sizes. *Inorganic Chemistry* **2012,** *51* (4), 2560-2568.

17.	Khan, A.; Nurnabi, M.; Bala, P., Studies on thermal transformation of Na–montmorillonite–glycine intercalation compounds. *Journal of Thermal Analysis and Calorimetry* **2009,** *96* (3), 929-935.

18.	Ohtsuka, K., Preparation and Properties of Two-Dimensional Microporous Pillared Interlayered Solids. *Chemistry of Materials* **1997,** *9* (10), 2039-2050.

19.	Laura, R. D.; Cloos, P., Adsorption of ethylenediamine (EDA) on montmorillonite saturated with different cations; III, Na-, K- and Li-montmorillonite; ion-exchange, protonation, co-ordination and hydrogen-bonding. *Clays and Clay Minerals* **1975,** *23* (1), 61-69.

20.	Bala, P.; Samantaraya, B. K.; Srivastava, S. K., Synthesis and characterization of Na-montmorillonite-alkylammonium intercalation compounds. *Materials Research Bulletin* **2000,** *35* (10), 1717-1724.

21.	Palvadeau, P.; Coic, L.; Rouxel, J.; Portier, J., The lithium and molecular intercalates of FeOCl. *Materials Research Bulletin* **1978,** *13* (3), 221-227.

22.   Benes, L.; Melanova, K.; Zima, V.; Kalousova, J.; Votinsky, J., Possible mechanisms of intercalation. *J. Inclusion Phenom. Mol. Recognit. Chem.* **1998,** *31* (Copyright (C) 2012 American Chemical Society (ACS). All Rights Reserved.), 275-286.

23.   Lin, J.-J.; Chen, Y.-M.; Yu, M.-H., Hydrogen-bond driven intercalation of synthetic fluorinated mica by poly(oxypropylene)-amidoamine salts. *Colloids and Surfaces A: Physicochemical and Engineering Aspects* **2007,** *302* (1–3), 162-167.

24.   Whittingham, M. S.; Jacobson, A. J.; Editors, *Intercalation Chemistry*. Academic Press: 1982; p 595 pp.

25.   Wang, G. J.; Qu, Q. T.; Wang, B.; Shi, Y.; Tian, S.; Wu, Y. P.; Holze, R., Electrochemical intercalation of lithium ions into LiV3O8 in an aqueous electrolyte. *Journal of Power Sources* **2009,** *189* (1), 503-506.

26.   NuLi, Y.; Yang, J.; Wang, J.; Li, Y., Electrochemical Intercalation of Mg2+ in Magnesium Manganese Silicate and Its Application as High-Energy Rechargeable Magnesium Battery Cathode. *The Journal of Physical Chemistry C* **2009,** *113* (28), 12594-12597.

27.   Feng, Z. Z.; Yang, J.; NuLi, Y. N.; Wang, J. L., *J. Power Sources* **2008,** *184*, 604.

28.   Feng, Z. Z.; Yang, J.; NuLi, Y. N.; Wang, J. L.; Wang, X. J., *Electrochem. Commun.* **2008,** *10*, 1291.

29.   Nalimova, V. A.; Sokolova, T. Y.; Avdeev, V. V.; Semenenko, K. N., Copper(II) chloride graphite intercalation compounds: phase transitions and interaction with alkali

metals at high pressure. *Materials Science Forum* **1992,** *91-93* (Intercalation Compd., Pt. 1), 401-6.

30.   Dresselhaus, M. S.; Dresselhaus, G., Intercalation compounds of graphite. *Adv. Phys.* **2002,** *51* (1), 1-186.

31.   Dresselhaus, M. S.; Dresselhaus, G., Intercalation compounds of graphite. *Advances in Physics* **1981,** *30* (2), 139-326.

32.   Zhao, W.; Tan, P. H.; Liu, J.; Ferrari, A. C., Intercalation of Few-Layer Graphite Flakes with FeCl3: Raman Determination of Fermi Level, Layer by Layer Decoupling, and Stability. *Journal of the American Chemical Society* **2011,** *133* (15), 5941-5946.

33.   Zhang, Y.; Scott, K. J.; Clearfield, A., Intercalation of alkylamines into layered copper phosphonates. *Chem. Mater.* **1993,** *5* (4), 495-499.

34.   Cao, G.; Hong, H. G.; Mallouk, T. E., Layered metal phosphates and phosphonates: from crystals to monolayers. *Accounts of Chemical Research* **1992,** *25* (9), 420-7.

35.   Cahen, S.; Vangelisti, R.; Bellouard, C., Structural and magnetic properties of a stage-2 HoCl3-graphite intercalation compound. *Carbon* **2006,** *44* (2), 259-266.

36.   Sun, L.; O'Reilly, J. Y.; Kong, D.; Su, J. Y.; Boo, W. J.; Sue, H. J.; Clearfield, A., The effect of guest molecular architecture and host crystallinity upon the mechanism of the intercalation reaction. *Journal of Colloid and Interface Science* **2009,** *333* (2), 503-509.

37.   Clearfield, A., Progress in Intercalation Research. In *Progress in Intercalation Research*, Müller-Warmuth, W.; Schollhorn, R., Eds. Kluwer: Dordrecht, 1994; pp 240-263.

38.   Kumar, C. V.; Bhambhani, A.; Hnatiuk, N., Layered a-zirconium phosphates and phosphonates. In *Handbook of Layered Materials*, Auerbach, S. M.; Carrado, K. A.; Dutta, P. K., Eds. Marcel Dekker, Inc.: New York, 2004; pp 313-372.

39.   Luzan, S. M.; Talyzin, A. V., Hydration of Graphite Oxide in Electrolyte and Non-Electrolyte Solutions. *J. Phys. Chem. C* **2011,** *115* (Copyright (C) 2012 American Chemical Society (ACS). All Rights Reserved.), 24611-24614.

40.   Hu, H.; Martin, J. C.; Xiao, M.; Southworth, C. S.; Meng, Y.; Sun, L., Immobilization of Ionic Liquids in Layered Compounds via Mechanochemical Intercalation. *Journal of Physical Chemistry C* **2011,** *115* (13), 5509-5514.

41.   Ogawa, M.; Hashizume, T.; Kuroda, K.; Kato, C., Intercalation of 2,2'-bipyridine and complex formation in the interlayer space of montmorillonite by solid-solid reactions. *Inorganic Chemistry* **1991,** *30* (3), 584-5.

42.   Bujdak, J.; Slosiarikova, H., The reaction of montmorillonite with octadecylamine in solid and melted state. *Applied Clay Science* **1992,** *7* (4), 263-269.

43.   Milanesio, M.; Conterosito, E.; Viterbo, D.; Perioli, L.; Croce, G., New Efficient Intercalation of Bioactive Molecules into Layered Double Hydroxide Materials by Solid-State Exchange: An in Situ XRPD Study. *Crystal Growth & Design* **2010,** *10* (11), 4710-4712.

44.   Wang, H.; Zou, M.; Li, N.; Li, K., Preparation and characterization of ionic liquid intercalation compounds into layered zirconium phosphates. *Journal of Materials Science* **2007,** *42* (18), 7738-7744.

45.   Khaorapapong, N.; Kuroda, K.; Hashizume, H.; Ogawa, M., Solid-state intercalation of 4,4′-bipyridine and 1,2-di(4-pyridine)ethylene into the interlayer spaces of Co(II)-, Ni(II)- and Cu(II)-montmorillonites. *Applied Clay Science* **2001,** *19* (1-6), 69-76.

46.   Ogawa, M.; Kato, K.; Kuroda, K.; Kato, C., Preparation of montmorillonite-alkylamine intercalation compounds by solid-solid reactions. *Clay Science* **1990,** *8* (1), 31-6.

47.   Clearfield, A.; Jirustithipong, P., Kinetics of gas-solid and solid-solid reactions in zirconium phosphate. *Fast Ion Transp. Solids: Electrodes Electrolytes, Proc. Int. Conf.* **1979**, 153-6.

48.   Ogawa, M.; Nagafusa, Y.; Kuroda, K.; Kato, C., Solid-state intercalation of acrylamide into smectites and Na-taeniolite. *Applied Clay Science* **1992,** *7* (4), 291-302.

49.   Vliers, D. P.; Collin, D.; Schoonheydt, R. A.; De Schryver, F. C., Synthesis and characterization of aqueous tris(2,2'-bipyridine)ruthenium(II)-zirconium phosphate suspensions. *Langmuir* **1986,** *2* (2), 165-169.

50.   Troup, J. M.; Clearfield, A., Mechanism of ion exchange in zirconium phosphates. 20. Refinement of the crystal structure of .alpha.-zirconium phosphate. *Inorganic Chemistry* **1977,** *16* (12), 3311-3314.

51. Clearfield, A.; Editor, *Inorganic Ion Exchange Materials*. CRC Press, Inc.: 1982; p 290 pp.

52. Martí, A. A.; Colón, J. L., Direct Ion Exchange of Tris(2,2'-bipyridine)ruthenium(II) into an α-Zirconium Phosphate Framework. *Inorganic Chemistry* **2003,** *42* (9), 2830-2832.

53. Clearfield, A.; Duax, W. L.; Medina, A. S.; Smith, G. D.; Thomas, J. R., Mechanism of ion exchange in crystalline zirconium phosphates. I. Sodium ion exchange of a-zirconium phosphate. *Journal of Physical Chemistry* **1969,** *73* (10), 3424-30.

54. Alberti, G.; Costantino, U.; Gill, J. S., Crystalline insoluble acid salts of tetravalent metals—XXIII: Preparation and main ion exchange properties of highly hydrated zirconium bis monohydrogen orthophosphates. *Journal of Inorganic and Nuclear Chemistry* **1976,** *38* (9), 1733-1738.

55. Kijima, T., Direct preparation of q-zirconium phosphate. *Bulletin of the Chemical Society of Japan* **1982,** *55* (9), 3031-2.

56. Kumar, C. V.; Williams, Z. J., Supramolecular Assemblies of Tris(2,2'-bipyridine)ruthenium(II) Bound to Hydrophobically Modified a-Zirconium Phosphate: Photophysical Studies. *Journal of Physical Chemistry* **1995,** *99* (49), 17632-9.

57. Martí, A. A.; Colón, J. L., Photophysical Characterization of the Interactions among Tris(2,2′-bipyridyl)ruthenium(II) Complexes Ion-Exchanged within Zirconium Phosphate. *Inorganic Chemistry* **2010,** *49* (16), 7298-7303.

58.   Marti, A. A.; Rivera, N.; Soto, K.; Maldonado, L.; Colon, J. L., Intercalation of Re(phen)(CO)3Cl into zirconium phosphate: a water insoluble inorganic complex immobilized in a highly polar rigid matrix. *Dalton Transactions* **2007,** (17), 1713-1718.

59.   Rivera, E. J.; Figueroa, C.; Colón, J. L.; Grove, L.; Connick, W. B., Room-Temperature Emission from Platinum(II) Complexes Intercalated into Zirconium Phosphate-Layered Materials. *Inorganic Chemistry* **2007,** *46* (21), 8569-8576.

60.   Díaz, A.; David, A.; Pérez, R.; González, M. L.; Báez, A.; Wark, S. E.; Zhang, P.; Clearfield, A.; Colón, J. L., Nanoencapsulation of Insulin into Zirconium Phosphate for Oral Delivery Applications. *Biomacromolecules* **2010,** *11* (9), 2465-2470.

61.   Santiago, M. E. B.; Declet-Flores, C.; Díaz, A.; Vélez, M. M.; Bosques, M. Z.; Sanakis, Y.; Colón, J. L., Layered Inorganic Materials as Redox Agents: Ferrocenium-Intercalated Zirconium Phosphate. *Langmuir* **2007,** *23* (14), 7810-7817.

62.   Sun, L.; Boo, W. J.; Browning, R. L.; Sue, H.-J.; Clearfield, A., Effect of Crystallinity on the Intercalation of Monoamine in α-Zirconium Phosphate Layer Structure. *Chemistry of Materials* **2005,** *17* (23), 5606-5609.

63.   Boo, W. J.; Sun, L.; Liu, J.; Clearfield, A.; Sue, H.-J., Effective Intercalation and Exfoliation of Nanoplatelets in Epoxy via Creation of Porous Pathways. *Journal of Physical Chemistry C* **2007,** *111* (28), 10377-10381.

64.   Kumar, C. V.; Chaudhari, A., Proteins Immobilized at the Galleries of Layered a-Zirconium Phosphate: Structure and Activity Studies. *Journal of the American Chemical Society* **2000,** *122* (5), 830-837.

65.   Kim, H.-N.; Keller, S. W.; Mallouk, T. E.; Schmitt, J.; Decher, G., Characterization of Zirconium Phosphate/Polycation Thin Films Grown by Sequential Adsorption Reactions. *Chemistry of Materials* **1997,** *9* (6), 1414-1421.

66.   Takei, T.; Kobayashi, Y.; Hata, H.; Yonesaki, Y.; Kumada, N.; Kinomura, N.; Mallouk, T. E., Anodic Electrodeposition of Highly Oriented Zirconium Phosphate and Polyaniline-Intercalated Zirconium Phosphate Films. *Journal of the American Chemical Society* **2006,** *128* (51), 16634-16640.

67.   Coronado, E.; Marti-Gastaldo, C.; Navarro-Moratalla, E.; Ribera, A.; Galan-Mascaros, J. R., Intercalation of two-dimensional oxalate-bridged molecule-based magnets into layered double hydroxide hosts. *Journal of Materials Chemistry* **2010,** *20* (42), 9476-9483.

68.   *Proteins at Interfaces II*. American Chemical Society: 1995; Vol. 602, p 580.

69.   Messing, R. A., *Immobilized enzymes for industrial reactors*. Academic Press: New York, 1975.

70.   Bertrand, P.; Jonas, A.; Laschewsky, A.; Legras, R., Ultrathin polymer coatings by complexation of polyelectrolytes at interfaces: suitable materials, structure and properties. *Macromolecular Rapid Communications* **2000,** *21* (7), 319-348.

71.   Patro, T. U.; Wagner, H. D., Layer-by-layer assembled PVA/Laponite multilayer free-standing films and their mechanical and thermal properties. *Nanotechnology* **2011,** *22* (45), 455706.

72.   Nakamura, T.; Ogawa, M., Attachment of the Sulfonic Acid Group in the Interlayer Space of a Layered Alkali Silicate, Octosilicate. *Langmuir* **2012,** *28* (19), 7505-7511.

73.   Van Rhijn, W. M.; De Vos, D. E.; Sels, B. F.; Bossaert, W. D.; Jacobs, P. A., *Chem. Commun.* **1998**, 317.

74.   Lim, M. H.; Blanford, C. F.; Stein, A., *Chem. Mater.* **1998,** *10*, 467.

75.   Molnar, B. R. A.; Forgoa, P.; Mohaib, M.; Bertoti, I., *J. Mol. Catal. A: Chem.* **2006,** *244*, 57.

76.   Melero, J. A.; Grieken, R.; Morales, G., *Chem. Rev.* **2006,** *106*, 3790.

CHAPTER II

PREPARATION OF INTERCALATED POLYMER/INORGANIC HYBRIDS VIA *IN SITU* SYNTHESIS

1. Introduction

Nanostructured organic-inorganic hybrid materials, including polymer nanocomposites and layer-by-layer assembled thin films, have been extensively investigated over the past two decades and have found wide applications owing to their excellent performance.[69, 76] Either regular polymer nanocomposites or layer-by-layer assembled thin films are prepared using pre-synthesized nanofillers/nanoplatelets. For polymer nanocomposites, huge efforts have been made on dispersing nanofillers into polymer matrices, owing to the inherent nature of nanofillers to agglomerate. However, a desirable state of dispersion is not necessarily achieved. For layer-by-layer assembled thin films, individual nanoplatelets must be pre-formed (exfoliated) before the assembly process. For most intercalation compounds, they are synthesized by intercalating the preformed layered materials.

Herein, we explore a new approach to prepare layered intercalation compounds via the *in situ* synthesis of layered compoundsin the presence of selected polymers, with an expectation that the selected polymers, which can generate weak interactions with the layered compounds, will be interacted into the layered materials to form layered

intercalated hybrids. Alpha-zirconium phosphate (α-ZrP), $Zr(HPO_4)_2 \cdot H_2O$, was selected as the base layered compound to be *in situ* synthesized to prepare intercalated hybrid materials.

2. Experimental and Materials

2.1 Materials

Zirconyl chloride octahydrate ($ZrOCl_2 \cdot 8H_2O$, 98%, Aldrich), phosphoric acid (85%, Aldrich), and polyethylene glycol (PEG) 400, 600, 1000, 1900, 4000, and 8000 (Alfa Aesar) were used as received. Polyvinylalcohol (PVA) 4-98 (molecular weight 27,000, 98% hydrolysis) and 4-88 (molecular weight 31,000, 88% hydrolysis) (Kuraray) were used. Polyethyleneimine (PEI) samples with an average molecular weight of 600, 1800, and 600,000 were obtained from Sigma-Aldrich.

2.2 Synthesis method

The ZrP based compounds were synthesized via a hydrothermal method.[77] A sample of 20% zirconyl chloride solution was mixed with pre-determined amount of PEG (or, PEI, PVA) with various molecular weights and H_3PO_4 with various concentrations in a sealed Teflon-lined pressure vessel and reacted at 100 °C for 24 hr. In a series of time controlled experiments, the reactions were conducted for 24, 48, 72 and 96 hr. After the reaction, the products were washed and collected by centrifugation three times. After that, the ZrP/polymers hybrids were dried at 70 °C for 24 hr. The dried samples were ground with an agate mortar and pestle into fine powders.

2.3 Characterization

X-ray diffraction (XRD) patterns were recorded on a Bruker D8 diffractometer with Bragg-Brentano θ-2θ geometry (20kV and 5 mA), using a graphite monochromator with Cu Kα radiation.

The thermal stability of the ZrP/PEG compounds were characterized by a thermogravimetric analyzer (TGA, TA Instruments model Q50) under an air atmosphere (40 mL/min) at a heating rate of 10 °C/min.

Scanning electron microscopy (SEM) images were acquired on a field emission-SEM (FE-SEM) from FEI (Helios Nanolab 400).

3. Results and Discussion

The synthesis of ZrP has been well investigated. Its morphology, crystallinity, and dimension can be tuned by controlling the synthesis conditions.[77] Thus, ZrP is an ideal layered compound for the preparation of polymer nanocomposites[62, 78] and intercalation chemistry research.[35, 61-62]

As expected, when PEG was added during the synthesis of ZrP, a ZrP/PEG intercalation compound formed. It is believed that during the growth of ZrP crystals, PEG molecules were embedded into the ZrP layers simultaneously, leading to the formation of an intercalation compound, as briefly illustrated by Figure 28.
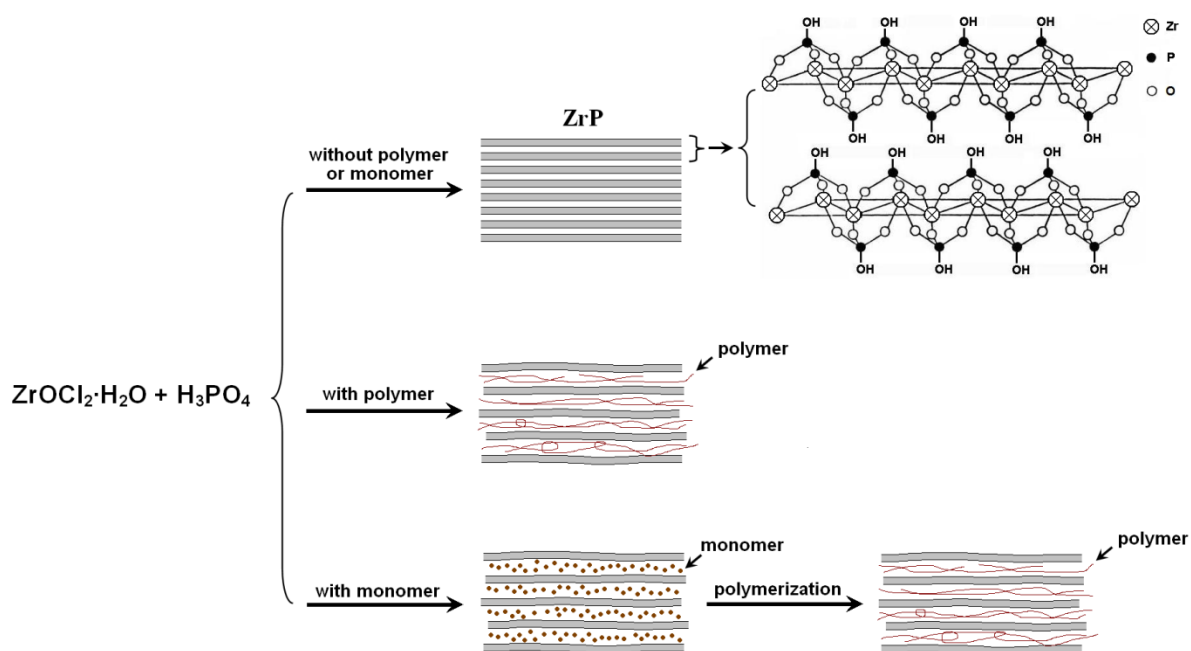
Figure 28. Schematic of the synthesis of ZrP with and without the presence of soluble

polymers/monomers.

By varying the weight ratio of ZrP to PEG600 (MW ca. 600) in the formulation

(assuming all Zr^{4+} cations converted to ZrP) from 4/1 to 1/4 at three different

concentration of H_3PO_4, the synthesized hybrid layered materials exhibiting different

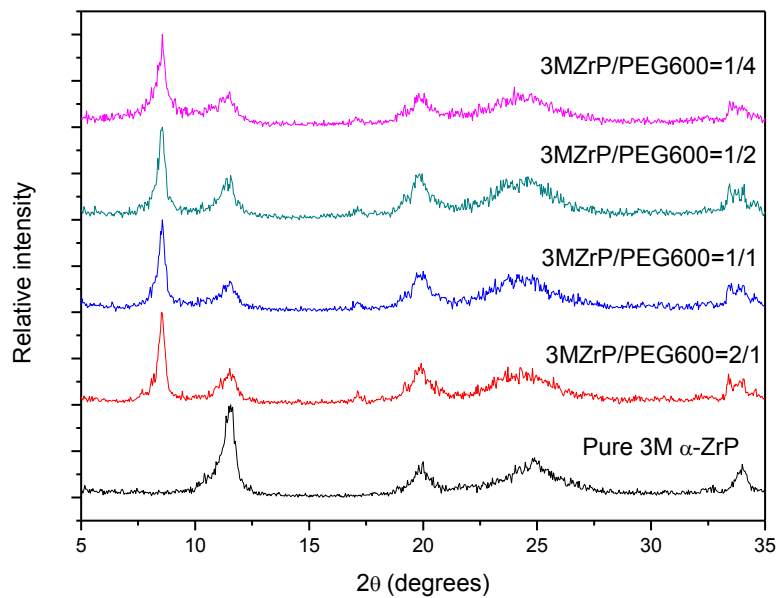morphologies and levels of crystallinity, as shown in Figures 29-31.

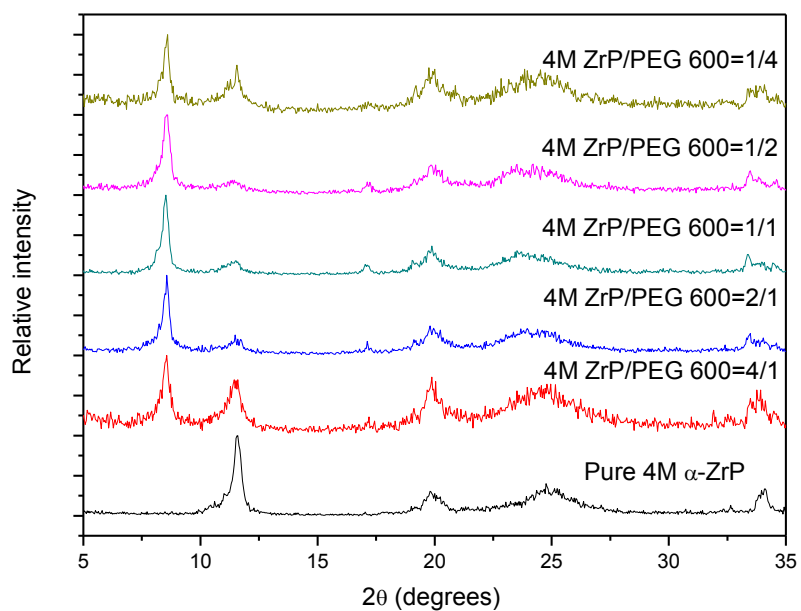**Figure 29**. XRD patterns of 3M ZrP/PEG600 with various formulation ratios.

Figure 30. XRD patterns of 4M ZrP/PEG600 with various formulation ratios.
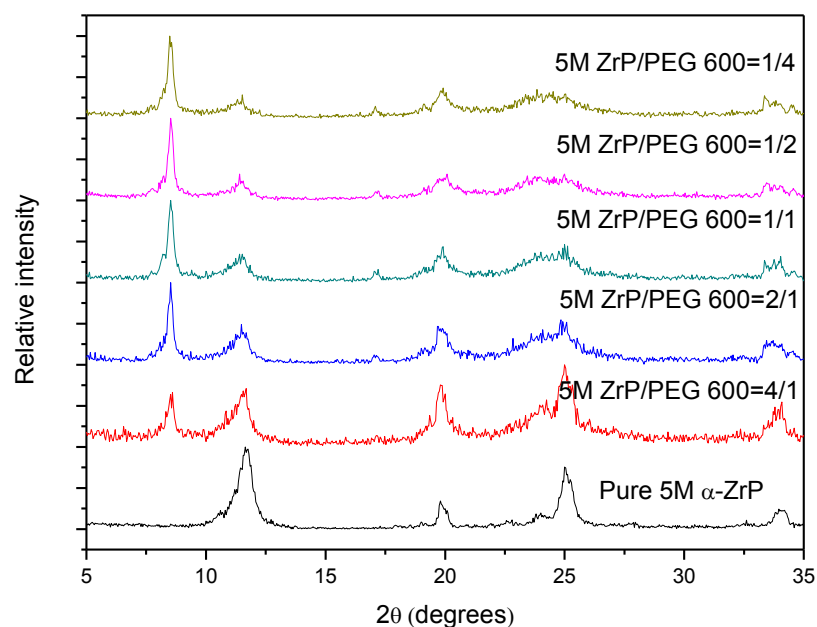
Figure 31. XRD patterns of 5M ZrP/PEG600 with various formulation ratios.

At all of the three concentration of H_3PO_4 (3M, 4M and 5M), when ZrP/PEG ratio is high, the product is a mixture of neat ZrP and ZrP/PEG intercalation compound. With increasing concentration of PEG in the formation, ZrP/PEG intercalation compound begins to dominate. The favored formation of ZrP/PEG intercalation compound over neat ZrP is expected. With a high concentration of PEG molecules in the ZrP synthesis environment, statistically such PEG chains will have a high chance to be embedded into the ZrP galleries.

The controlling of crystal size of ZrP was well developed years ago.[5] The more ordered and larger crystal size of ZrP crystals were synthesized in a higher concentration of phosphoric acid. Figure 32 shows the XRD patterns of samples synthesized under different acid concentrations under the same reaction condition with the same ZrP to PEG600 weight ratio. The results showed that the concentration of phosphoric acid has

marginal influences for the *in-situ* synthesized intercalation compounds. This indicated

that the size of ZrP crystals plays a less important role during the synthesis of

intercalation compound.
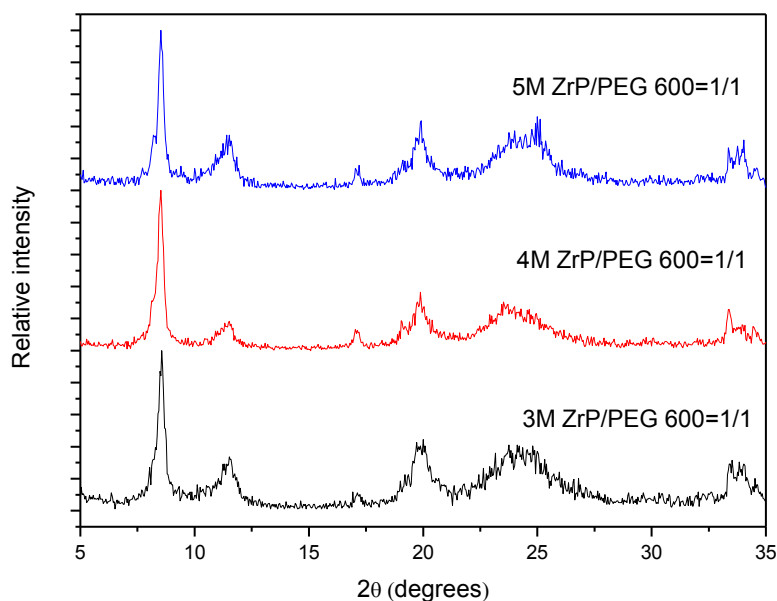
Figure 32. XRD patterns of ZrP/PEG600=1/1 with various phosphoric acid
concentration.

Reaction time is another parameter which may influence the product of intercalation

compound. Figure 33 shows the XRD patterns of intercalation compounds that

synthesized after different duration of reaction of 24, 48, 72 and 96 hr. Mixtures of

ZrP/PEG intercalation compounds and neat ZrP were found in all the products after

different reaction durations. These results showed that the reaction time is not an

important factor for the formation of intercalation compounds.

For all the ZrP/PEG intercalation compounds discussed above, their interlayer distance remains to be 10.4 Å, regardless of the ZrP/PEG concentration. This phenomenon will be discussed in detail later.
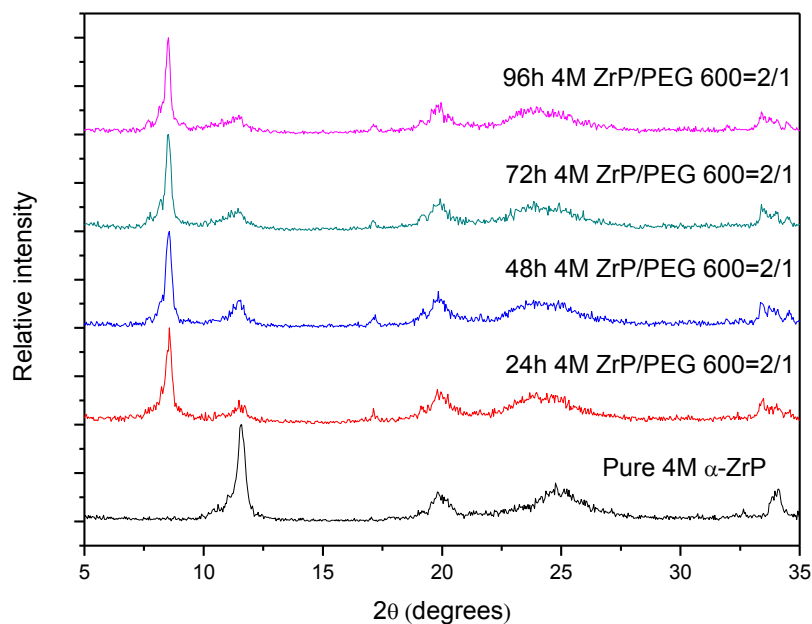
Figure 33. XRD patterns of 4M ZrP/PEG600=2/1 with various reaction time.

When PEG1900 was used during the synthesis of ZrP/PEG intercalation compounds, it was found that a much lower concentration of neat ZrP formed. Even at a ZrP/PEG weight ratio of 4:1, only a tiny amount of neat ZrP formed. When the PEG/ZrP weight ratio was raised to 50%, no neat ZrP was detected by XRD, as shown in Figure 34. Again, the interlayer distance of ZrP/PEG1900 intercalation compounds remains to be 10.4 Å.

Figure 34. XRD patterns of 4M ZrP/PEG1900 with various formulation ratios.

PEG macromolecules with varying MWs were used for the synthesis to investigate the effect of polymer chain length on the formation of ZrP/PEG intercalation co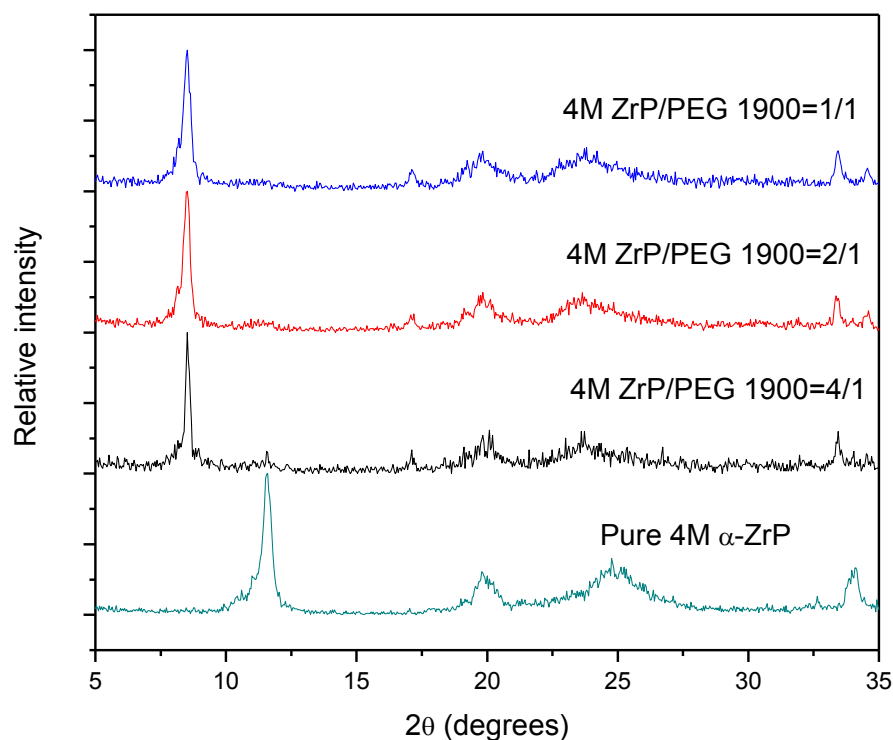mpounds. The XRD patterns are presented in Figure 35, which show that longer polymer chains are more effective to minimize the formation of pristine ZrP. While statistically chains with different lengths may have the similar chance to be anchored and embedded within the layers, the longer ones, once anchored, would affect a larger domain of intercalated structure. Thus overall, a longer PEG chain is favorable to help minimize the formation of neat ZrP.

It was observed that the PEG molecules with different chain lengths lead to the same interlayer distance of ZrP/PEG intercalation compounds, which is 10.4 Å. Together with

the observation from Figures 29 and 31, it shows that neither the concentration, nor the chain length of PEG, would affect the interlayer distance of the synthesized PEG/ZrP intercalation compounds. This suggests that PEG chains must be perfectly parallel to the layer planes. Simple modeling using Chem3D Pro shows that the PEG chain has a thickness of ca. 2.8 Å. This leads to an excellent agreement with the interlayer distance difference between ZrP (7.6 Å) and PEG/ZrP intercalation compounds (10.4 Å), indicating that only one layer of PEG chains are embedded into ZrP galleries, probably together with some hydrations.
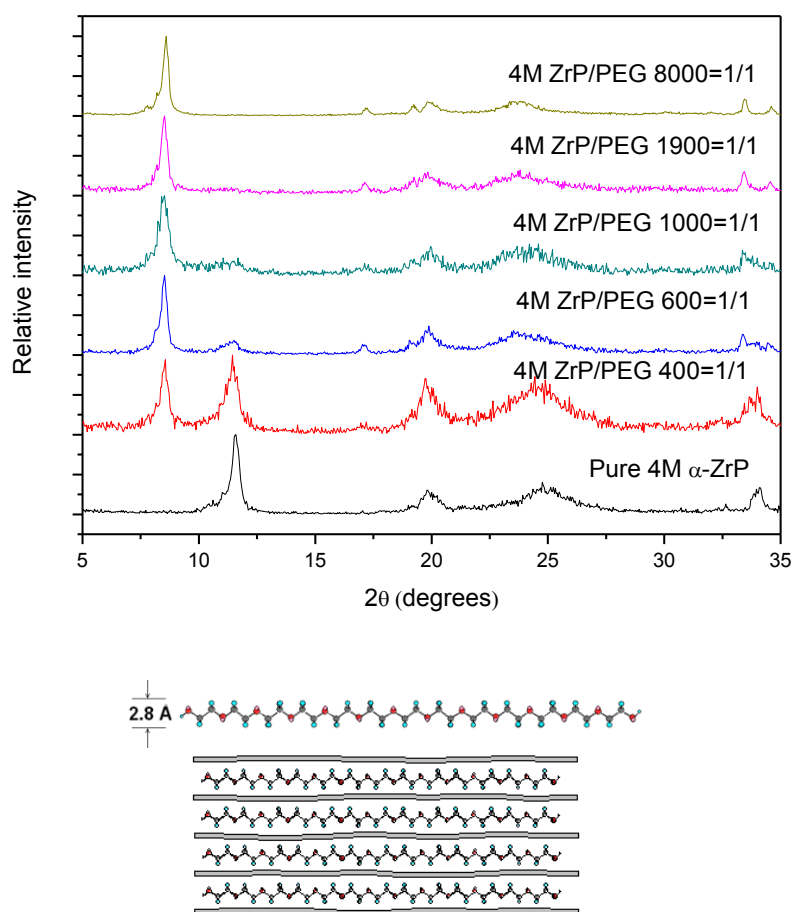

Figure 35. XRD patterns of ZrP/PEG intercalation compounds containing PEG with varying MWs at ZrP/PEG=1/1 and PEG, ZrP/PEG model.

To further prove that PEG was indeed embedded into the ZrP layers during the formation of ZrP crystals, instead of being intercalated into the formed ZrP, a control experiment was carried out and the results were shown in Figure 36. A series of neat ZrP samples in 3.0, 4.0 and 5.0 M molarity of phosphoric acid were first synthesized under the same conditions to synthesize the above intercalation compounds, whose XRD patterns are shown in Figure 9. Subsequently, PEG600 was added, and then reacted under the same hydrothermal reaction condition for 24 hours. The final products were collected and dried for XRD. The results show that no PEG was intercalated into the pre-formed ZrP. This proves that PEG cannot be intercalated into any pre-synthesized ZrP micro-crystals via regular intercalation procedures, which in turn suggests ZrP/PEG intercalation compounds should be formed *in situ* as this project designed.
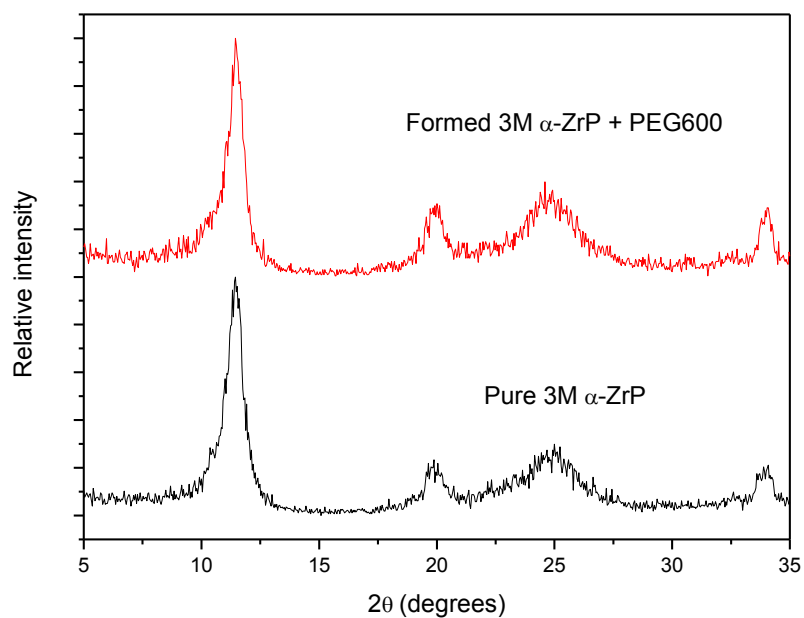

Figure 36. XRD patterns of the sample synthesized from attempted intercalation between the pre-synthesized ZrP and PEG600 under different concentrations of H_3PO_4.
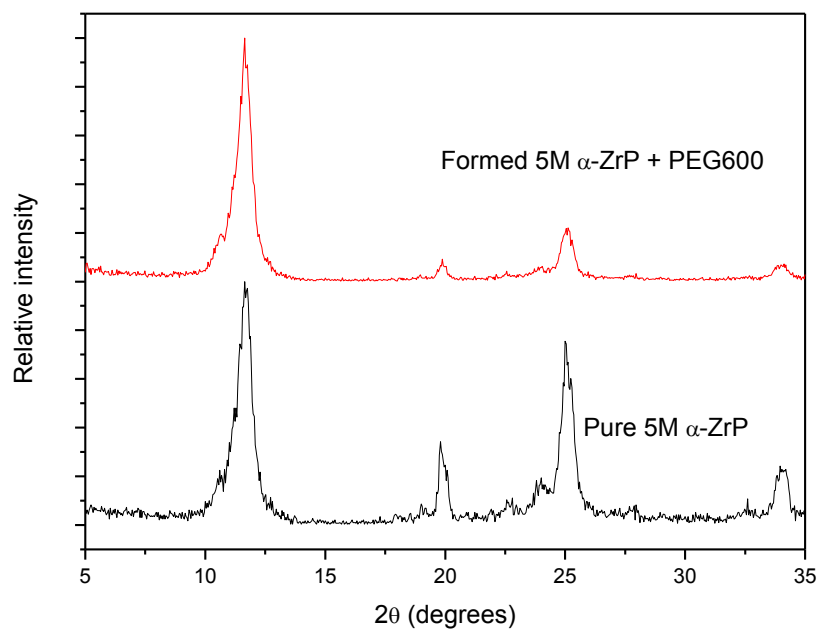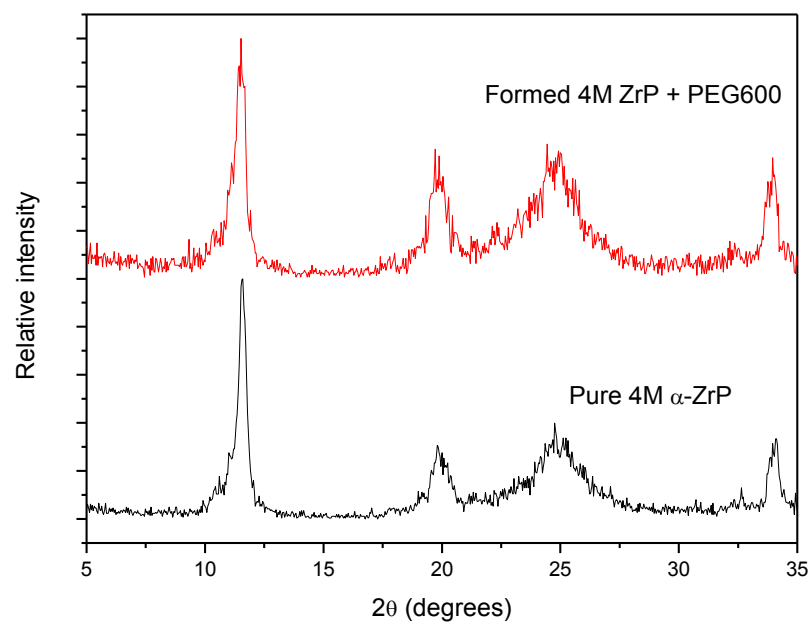
Figure 36. **continued**

SEM imaging was performed on selected intercalation compounds. Figure 37 shows different molecular weights of PEG in same hybrid weight ratio. The intercalation compounds exhibit a similar crystal size as the neat ZrP synthesized under the same conditions which is around 100nm-120nm period. Figure 38 shows the ZrP/PEG1000 intercalation compounds with different ZrP/PEG ratios. Similarly, such intercalation compounds also exhibited close crystal size as the pristine ZrP control. The results indicate that either the molecular weight or the concentration of guest polymer hardly influences the size of the formed intercalation compounds.

Figure 37. SEM image of : (A) pristine 4M-100°C-24h ZrP. (B) ZrP/PEG400=1:1interclation compound. (C) ZrP/PEG600=1:1interclation compound. (D) ZrP/PEG1000=1:1interclation compound. (E) ZrP/PEG1900=1:1interclation compound. (F) ZrP/PEG8000=1:1interclation compound.

68
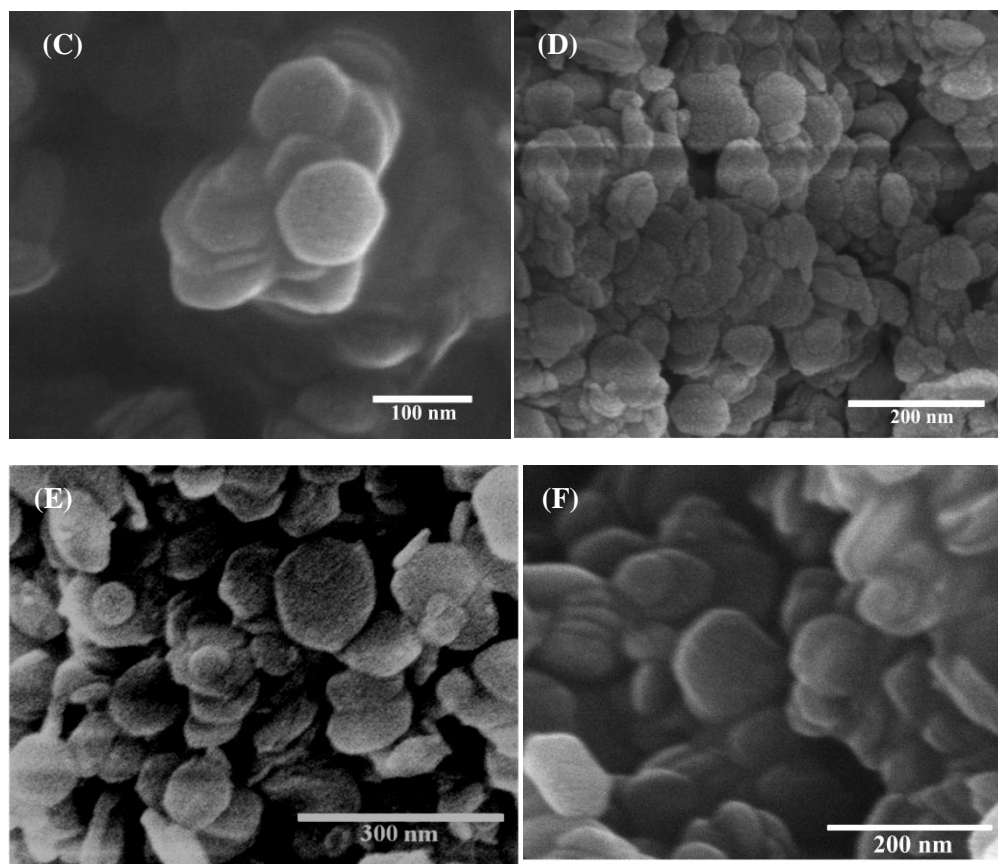
Figure 37. **continued**
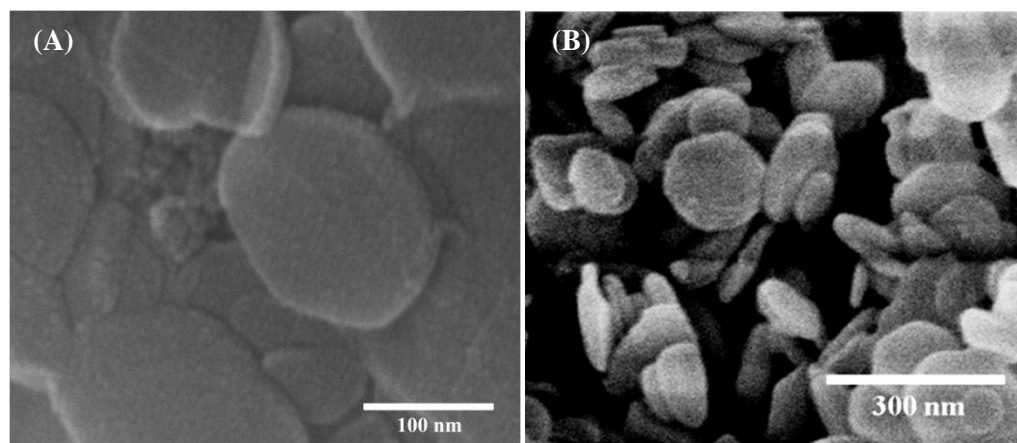
Figure 38. SEM image of : (A) pristine 4M-100°C-24h ZrP. (B)
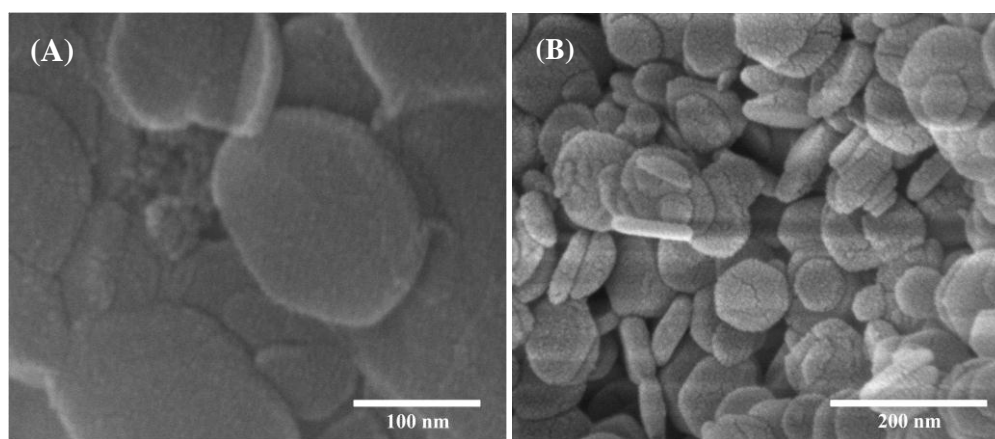
ZrP/PEG1000=4:1interclation compound. (C) ZrP/PEG1000=2:1interclation compound.

(D) ZrP/PEG1000=1:1interclation compound. (E) ZrP/PEG1000=1:2interclation

compound. (F) ZrP/PEG1000=1:4interclation compound.
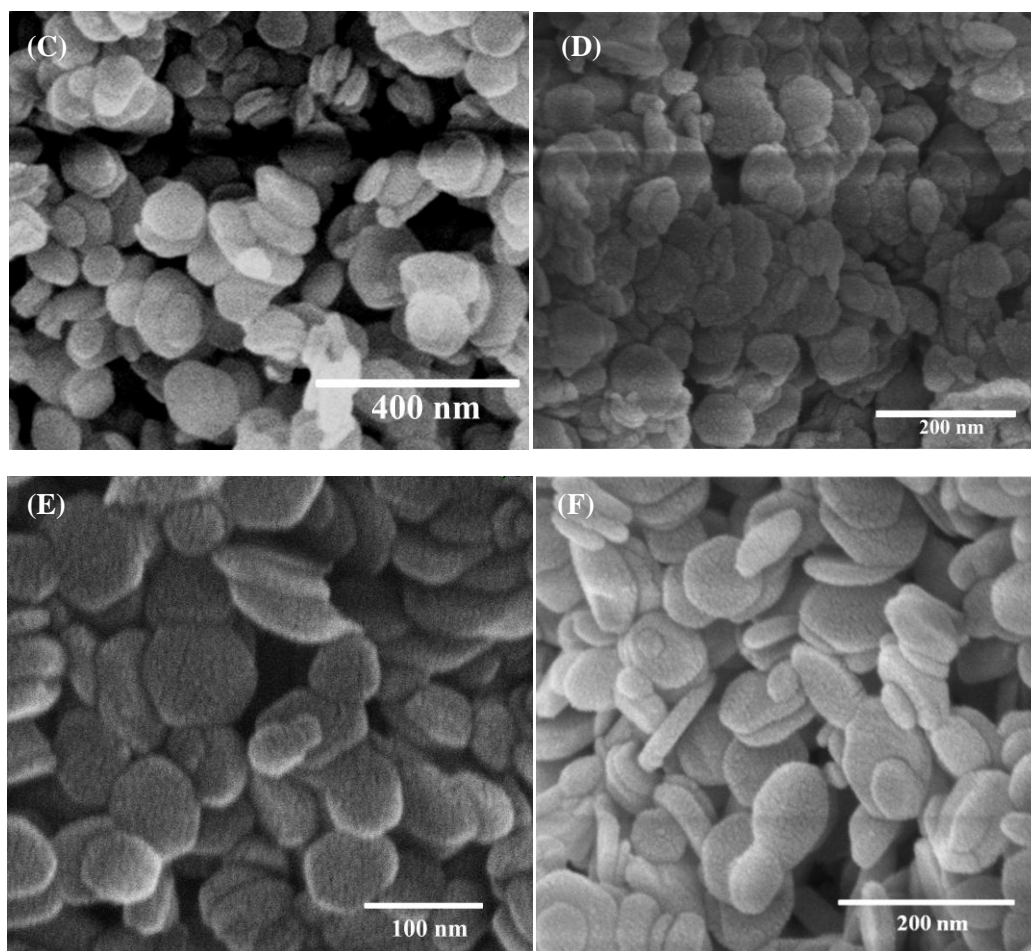
Figure 38. **continued**

Figure 39 shows the SEM images of the ZrP crystals synthesized using 3.0, 4.0, and

5.0 M H3PO4, versus the ZrP/PEG intercalation compounds synthesized under the same

reaction condition. The images show that with the increasing concentration of H_3PO_4, the

average crystal size increases. Correspondingly, the crystal size of the intercalation

compounds increased as well. Again, the crystal size of intercalated ZrP is similar to that

of the pristine ones. For example, in Figure 39, the crystal sizes of the pristine 3M ZrP

and the ZrP/PEG intercalation compound are similar (ca. 90 nm). These phenomena were

also found in the cases of 4 M and 5 M samples.
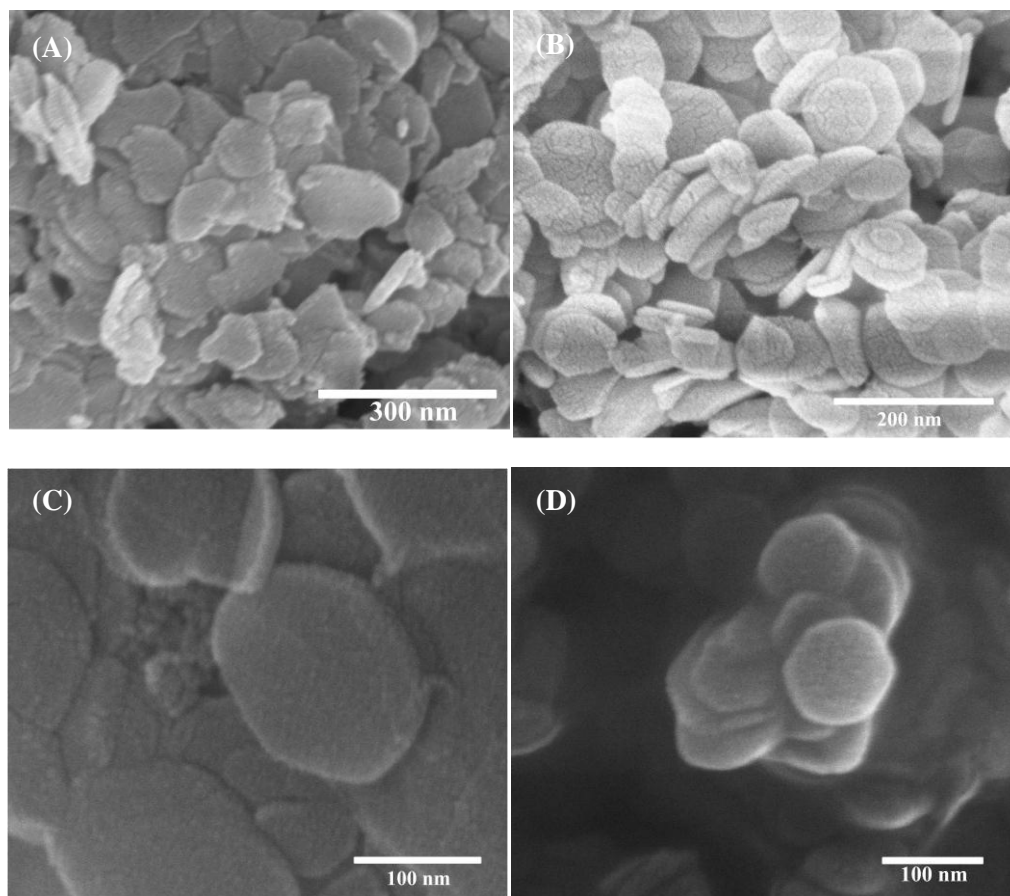
Figure 39. SEM image of :(A) pristine 3M-100°C-24h ZrP. (B) 3M

ZrP/PEG600=1:1interclation compound. (C) pristine 4M-100°C-24h ZrP. (D) 4M

ZrP/PEG600=1:1interclation compound. (E) pristine 5M-100°C-24h ZrP. (F) 5M

ZrP/PEG600=1:1interclation compound.
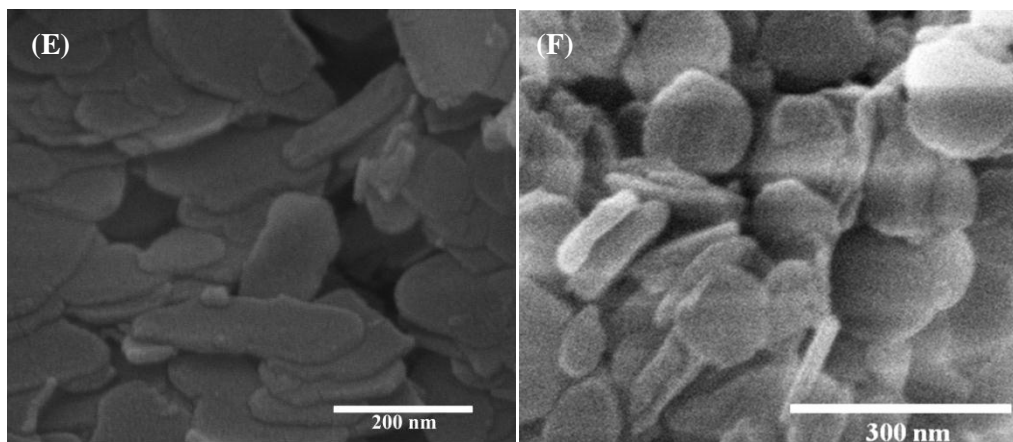
Figure 39. continued

Thermogravometric analyses were also performed on the selected intercalation compounds. As shown in Figure 40, the degradation of PEG600 in PEG600/ZrP interclation compound was slightly delayed compared to the neat PEG600. Such a delayed degrdation is belived to be due to either the extra bondings to be broke for ZrP with PEG rather than PEG chains themselves or the protection effect produced by ZrP layer sheets. The TGA result also suggested that the PEG/ZrP intercalation compound contains ca. 12% PEG.
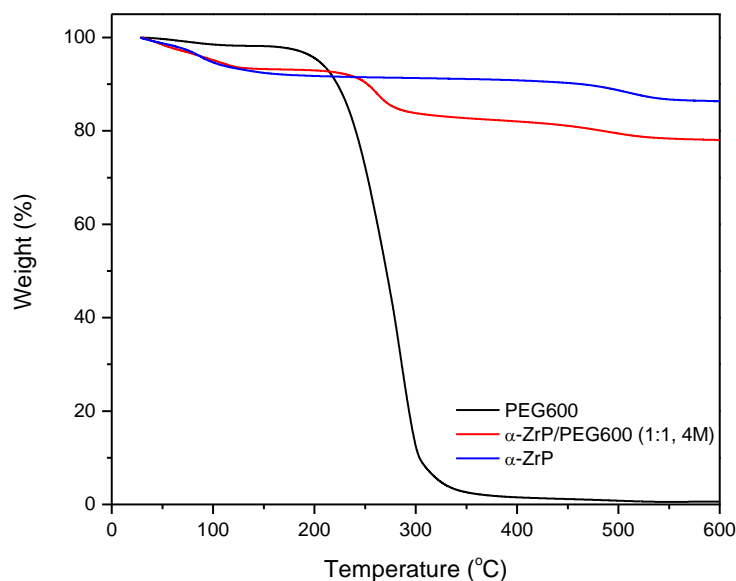
Figure 40. TGA analysis of PEG600, neat ZrP, and PEG600/ZrP intercalation

compounds.

In addition to ZrP/PEG intercalation compounds, PVA was also tested with the same

synthesis procedure as PEG samples. PVA samples were classified into two series: one is

PVA with 98% hydrolysis; the other group was 88% hydrolysis. Figures 41 and 42 show

that 98% hydrolysis or 88% hydrolysis PVA performed very similarly in the reaction.

And the overall reaction trend in terms of the ratio of the intercalation compound and the

neat ZrP are very similar to the ZrP/PEG intercalation compounds: a higher concentration

of polymer led to a more complete formation of the intercalation compounds. The

interlayer distance also remained the same. It also provided information that the

percentage of hydrolysis does not influence the intercalation.
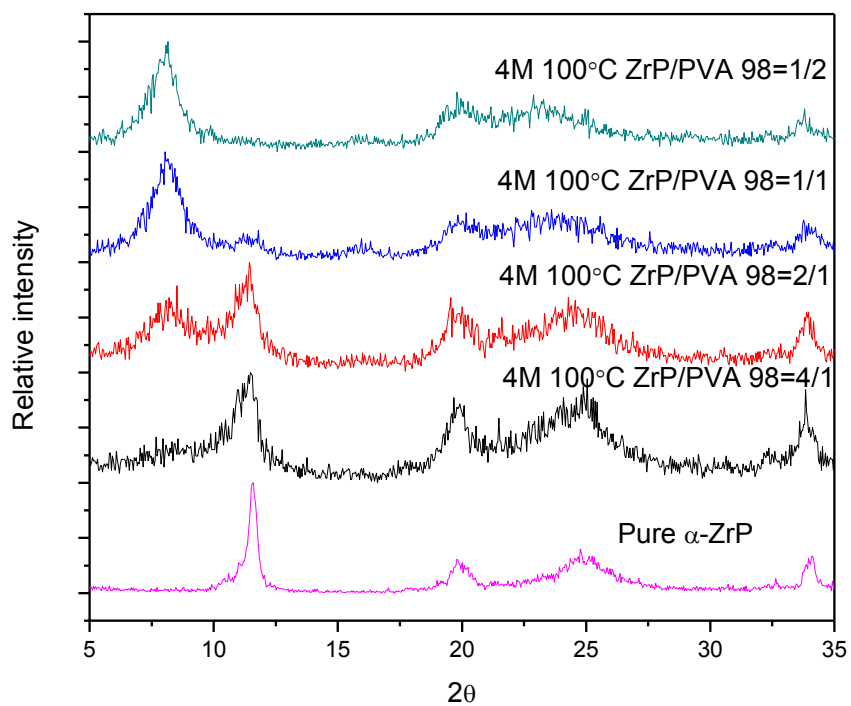
Figure 41. XRD patterns of the ZrP/PVA 4-98 intercalation compounds in different
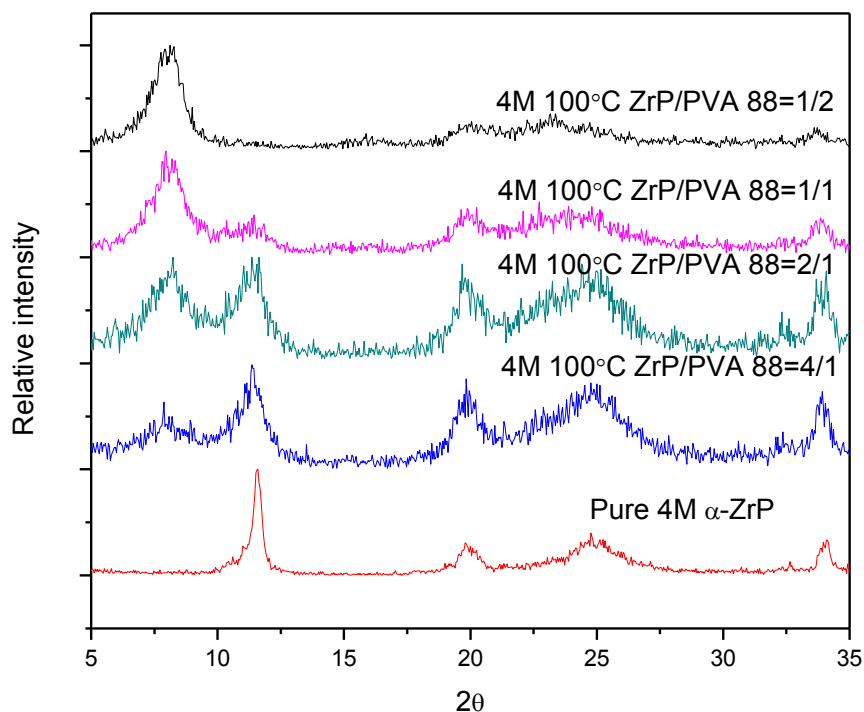
ZrP/PVA ratio.

Figure 42. XRD patterns of the ZrP/PVA 4-88 intercalation compounds in different

ZrP/PVA ratio.

   Since the synthesis of ZrP is conducted under an acidic condition, some polymers,

such as PVA, are very easy to decompose. As a result, the synthesis reactions in a

relatively low concentration of acid and at low temperature were also carried out to

prevent polymer degradation. Figure 43 shows the ZrP/PVA 4-98 intercalation

compounds synthesized using 3 M phosphoric acid at 65 °C. In comparison with Figure

14, the 3M ZrP/PVA 4-98 65°C intercalation compound contains less pristine ZrP than

the sample synthesized at 100°C. This indicates that temperature plays an important role

for the synthesis. One explanation is that at a lower synthesis temperature, the ZrP

formation rate tends to be slower. Consequently, it offers a higher possibility for guest

polymers to be embedded into the galleries during the *in situ* synthesis.
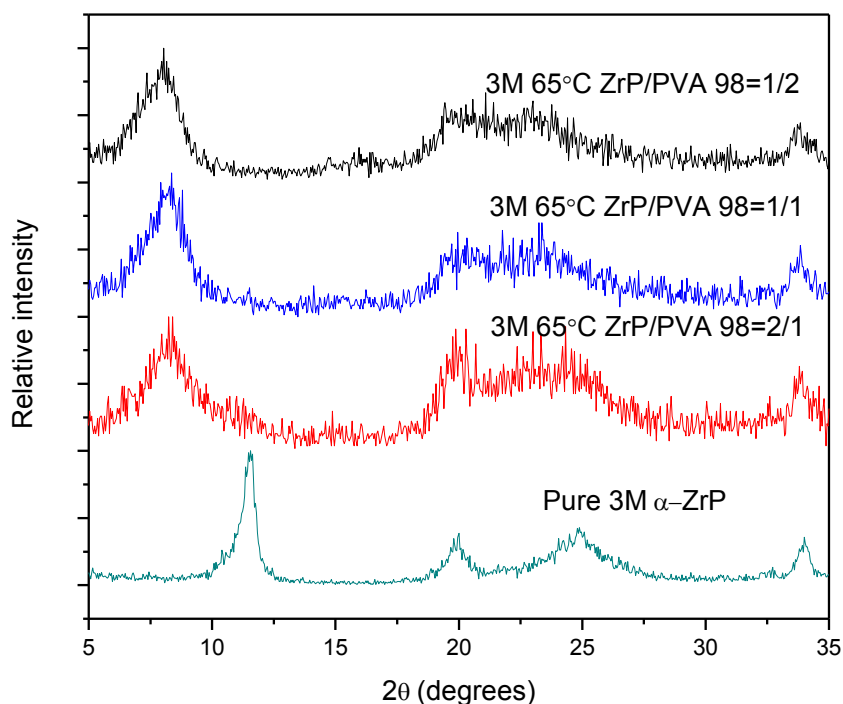
Figure 43. XRD patterns of the 3M ZrP/PVA 4-98 intercalation compounds in different

ZrP/PVA ratio react under 65°C.

Another guest polymer PEI was also successfully synthesized with ZrP by this

method to produce ZrP/PEI intercalation compound. The results presented in Figure 44

show a great similarity as ZrP/PEG and ZrP/PVA intercalation compounds.
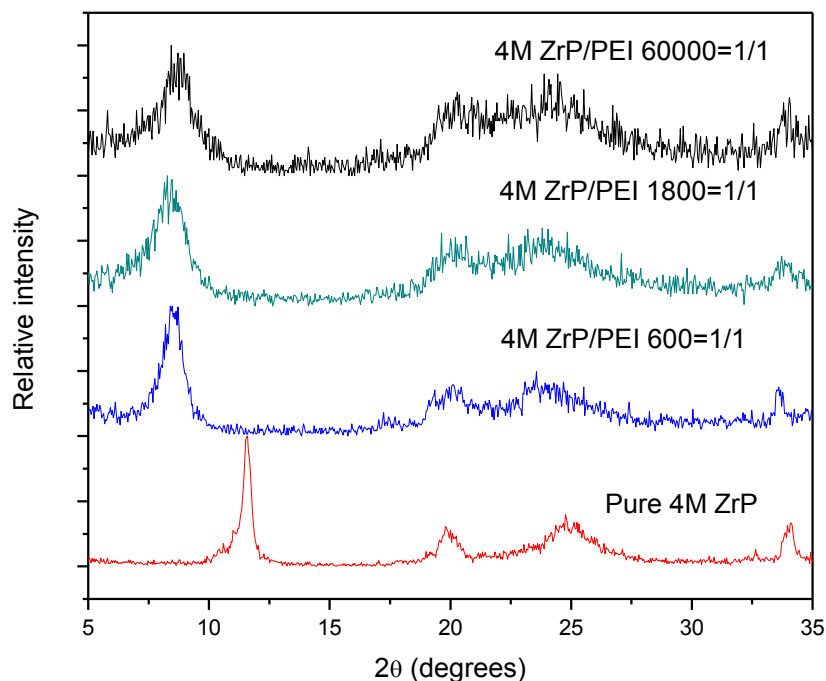
Figure 44. XRD patterns of the 4M ZrP/PEI intercalation compounds in different PEI

molecular weight.

4. Conclusions

Overall, our results have shown that the in situ synthesis approach to directly prepare

layered intercalation compounds is able to directly produce layered intercalation

compound instead of traditional intercalation methods. A high concentration of guest

molecules and a higher molecular weight polymer are favorable for the formation of the

layered intercalation compounds. The presence of guest polymer does not affect the

dimension of the formed intercalation compounds, regardless of their concentration or

molecular weight. In addition, the guest molecules are well confined within the layers, as

all the guest polymer chains are all well aligned and parallel within the formation

intercalation compounds.

The preliminary results have shown that *in situ* synthesis can be an effective and efficient approach to prepare nanostructured composite materials. Such nanostructured composite materials can not only find applications as regular nanocomposites, may also find applications in sensors, drug delivery, coatings, or as a new platform to study the behavior of polymers which are constrained in layers.

References

1. (a) Giannelis, E. P., Polymer layered silicate nanocomposites. *Advanced Materials* **1996,** *8* (1), 29-35; (b) Alexandre, M.; Dubois, P., Polymer-layered silicate nanocomposites: preparation, properties and uses of a new class of materials. *Materials Science & Engineering R-Reports* **2000,** *28* (1-2), 1-63; (c) Winey, K. I.; Vaia, R. A., Polymer nanocomposites. *MRS Bulletin* **2007,** *32* (4), 314-319; (d) Bertrand, P.; Jonas, A.; Laschewsky, A.; Legras, R., Ultrathin polymer coatings by complexation of polyelectrolytes at interfaces: suitable materials, structure and properties. *Macromolecular Rapid Communications* **2000,** *21* (7), 319-348.

2. Sun, L.; Boo, W. J.; Sue, H.-J.; Clearfield, A., Preparation of α-zirconium phosphate nanoplatelets with wide variations in aspect ratios. *New Journal of Chemistry* **2007,** *31* (1), 39-43.

3. (a) Sue, H.-J.; Gam, K. T.; Bestaoui, N.; Spurr, N.; Clearfield, A., Epoxy nanocomposites based on the synthetic α-zirconium phosphate layer structure. *Chemistry of Materials* **2004,** *16* (2), 242-249; (b) Sue, H.-J.; Gam, K. T.; Bestaoui, N.; Clearfield, A.; Miyamoto, M.; Miyatake, N., Fracture behavior of a-zirconium phosphate-based epoxy nanocomposites. *Acta Materialia* **2004,** *52* (8), 2239-2250; (c) Sun, L.; Boo, W. J.; Sun, D.; Clearfield, A.; Sue, H.-J., Preparation of Exfoliated Epoxy/α-Zirconium Phosphate Nanocomposites Containing High Aspect Ratio Nanoplatelets. *Chemistry of Materials* **2007,** *19* (7), 1749-1754; (d) Boo, W. J.; Sun,

L.; Liu, J.; Clearfield, A.; Sue, H.-J., Effective Intercalation and Exfoliation of Nanoplatelets in Epoxy via Creation of Porous Pathways. *Journal of Physical Chemistry C* **2007,** *111* (28), 10377-10381; (e) Boo, W. J.; Sun, L.; Liu, J.; Clearfield, A.; Sue, H.-J.; Mullins, M. J.; Pham, H., Morphology and mechanical behavior of exfoliated epoxy/α-zirconium phosphate nanocomposites. *Composites Science and Technology* **2007,** *67* (2), 262-269; (f) Boo, W. J.; Sun, L.; Liu, J.; Moghbelli, E.; Clearfield, A.; Sue, H.-J.; Pham, H.; Verghese, N., Effect of Nanoplatelet Dispersion on Mechanical Behavior of Polymer Nanocomposites. *Journal of Polymer Science, Part B: Polymer Physics* **2007**, 1459-1469; (g) Boo, W. J.; Sun, L.; Warren, G. L.; Moghbelli, E.; Pham, H.; Clearfield, A.; Sue, H.-J., Effect of nanoplatelet aspect ratio on mechanical properties of epoxy nanocomposites. *Polymer* **2007,** *48* (4), 1075-1082; (h) Sun, L.; Boo, W. J.; Clearfield, A.; Sue, H.-J.; Pham, H. Q., Barrier properties of model epoxy nanocomposites. *Journal of Membrane Science* **2008,** *318* (1-2), 129-136; (i) Sun, L.; Boo, W.-J.; Liu, J.; Clearfield, A.; Sue, H.-J.; Verghese, N. E.; Pham, H. Q.; Bicerano, J., Effect of Nanoplatelets on the Rheological Behavior of Epoxy Monomers. *Macromolecular Materials and Engineering* **2009,** *294* (2), 103-113; (j) Moghbelli, E.; Sun, L.; Jiang, H.; Boo, W. J.; Sue, H.-J., Scratch behavior of epoxy nanocomposites containing alpha-zirconium phosphate and core-shell rubber particles. *Polymer Engineering and Science* **2009,** *49* (3), 483-490; (k) Sun, L.; Liu, J.; Kirumakki, S. R.; Schwerdtfeger, E. D.; Howell, R. J.; Al-Bahily, K.; Miller, S. A.; Clearfield, A.; Sue, H.-J., Polypropylene Nanocomposites Based on Designed Synthetic Nanoplatelets. *Chemistry of Materials* **2009,** *21* (6), 1154-1161; (l) Sun, L.; Sue, H.-J., Permeation Properties of Epoxy Nanocomposites. In *Barrier Properties of*

Polymer Clay Nanocomposites, Mittal, V., Ed. Nova Science Publishers: New York, USA, 2010; pp 73-93.

4.   (a) Sun, L.; Boo, W. J.; Browning, R. L.; Sue, H.-J.; Clearfield, A., Effect of Crystallinity on the Intercalation of Monoamine in α-Zirconium Phosphate Layer Structure. *Chemistry of Materials* **2005,** *17* (23), 5606-5609; (b) Sun, L.; O'Reilly, J. Y.; Kong, D.; Su, J. Y.; Boo, W. J.; Sue, H. J.; Clearfield, A., The effect of guest molecular architecture and host crystallinity upon the mechanism of the intercalation reaction. *Journal of Colloid and Interface Science* **2009,** *333* (2), 503-509.

CHAPTER III

SYNTHESIS OF INTERCALATED ORGANIC/INORGANIC HYBRIDS VIA

LAYERED MATERIALS/MONOMER *IN SITU* SYNTHESIS

1. **Introduction**

Nowadays, out of cost, time, and energy consideration, simplification in synthesis

attracts more and more attention. In the synthesis of layered intercalation compounds,

many complicated intercalation strategies have been developed to intercalate guest

materials that have weak driving force or large dimension to achieve intercalation, such

as multistep intercalation method[79,80,81], exfoliation and reassembling strategy[82,66,68,65], or

layer-by-layer approach[70,69]. In chapter 2, via the in situ synthesis of ZrP in the presence

of selected polymers, ZrP/polymers intercalated compounds were successfully prepared.

The new strategy that directly synthesizes layered intercalation compounds instead of

intercalating the pre-formed layered materials has proved to achieve intercalation.

In this chapter, a more innovative idea that directly synthesizes layered intercalation

compounds through the synthesis of layered materials in the presence of polymerizable

monomers is explored. In this way, synthesis of a layered material, intercalation of the

layered material, and the polymerization of monomers can be completed in one pot and

within a single step. It can not only solve the cost, time, and energy issues, but also

provide a new strategy to generate organic/inorganic layered intercalation hybrids, especially for those polymers that hard to be direct intercalated.

2. Experimental and materials

2.1 Materials

Zirconyl chloride octahydrate ($ZrOCl_2 \cdot 8H_2O$, 98%, Aldrich), phosphoric acid (85%, Aldrich), and acrylamide monomer (TCI America) were used as received.

2.2 Synthesis method

The ZrP based compound was synthesized via a hydrothermal method.[77] A sample of 20% zirconyl chloride solution was mixed with pre-determined amount of acrylamide and H_3PO_4 with various concentrations in a sealed Teflon-lined pressure vessel and reacted at 100°C for 24 hr. After the reaction, the products were washed and collected by centrifugation three times. After that, the intercalation compounds were dried at 70 °C for 24 hr. The dried samples were ground with an agate mortar and pestle into fine powders.

2.3 Characterizations

X-ray diffraction (XRD) patterns were recorded on a Bruker D8 diffractometer with Bragg-Brentano θ-2θ geometry (20kV and 5 mA), using a graphite monochromator with Cu Kα radiation.

FTIR spectra were recorded on a Perkin Elmer Frontier FT-NIR/MIR Spectrometers. All the samples were mixed with KBr and further pressed as a pellet.

The thermal stability of the intercalation compounds were characterized by a thermogravimetric analyzer (TGA, TA Instruments model Q50) under an air atmosphere (40 mL/min) at a heating rate of 10 °C/min.

3. Results and discussion

The synthesis of ZrP/acrylamide intercalation compounds follows the same procedures of the synthesis of ZrP/PEG intercalation compounds. It is expected that acrylamide will be intercalated into ZrP interlayer space during the synthesis. Considering acrylamide can be heat polymerized into poly acrylamide (PAM) with the addition of acrylamide during the synthesis of ZrP, ZrP/acrylamide and/or ZrP/polyacrylamide intercalation compounds might be synthesized. By varying the weight ratio of ZrP to acrylamide monomers in the formulation (assuming all Zr^{4+} cations converted to ZrP) from 4/1 to 1/4, the synthesized hybrid layered materials exhibited different morphologies and levels of crystallinity, as shown in Figure 45.
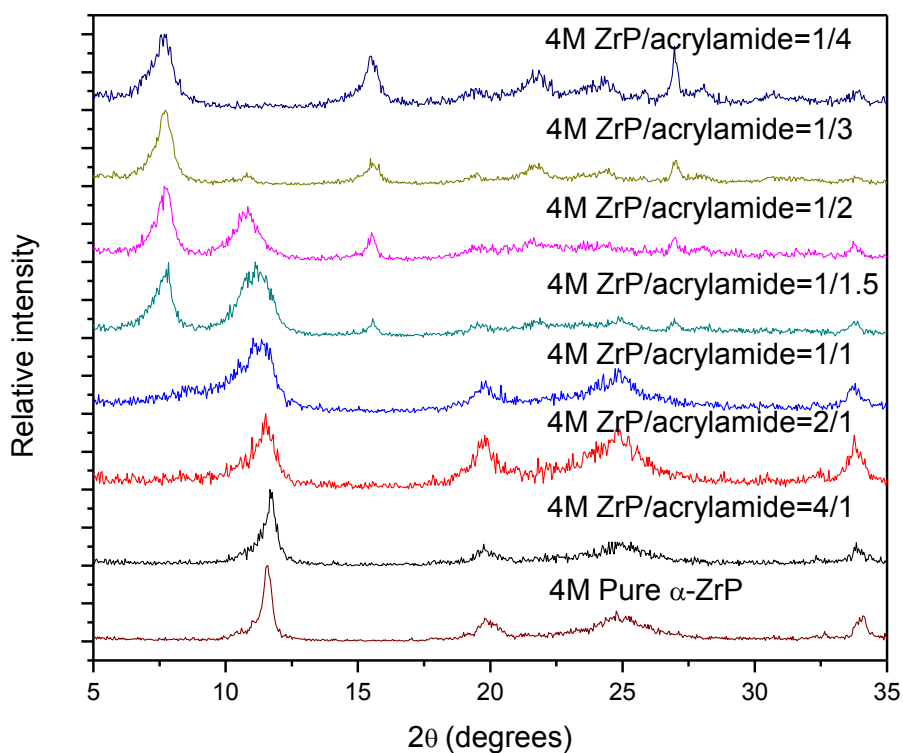

Figure 45. XRD patterns of ZrP/acrylamide in different formulation ratio.

When the weight ratio of ZrP to acrylamide is low, from 4/1 to 1/1, the products were mostly dominated by neat ZrP. According to the result in chapter 2, at low ratios of PEG/ZrP ratio in the case of low molecular weight of PEG, a mixture of ZrP and ZrP/PEG were synthesized. In contrast, at low acrylamide/ZrP ratios, virtually no intercalation compounds were formed. This is probably owing to the low molecular weight of acrylamide. Base on the result in Chapter 2, the PEG with a larger molecular weight are easier to be embedded into ZrP galleries. This suggests that monomers are difficult to be embedded within the interlayer space through this in situ synthesis method.

With the increasing acrylamide/ZrP weigh ratio, the products showed an increasing concentration of intercalation compounds compared to the neat ZrP. When the mass ratio of ZrP/acrylamide was increased to 1/4, no neat ZrP was detected by XRD. Eventually, similar intercalation has been achieved as the ZrP/PEG examples discussed in Chapter 2.

In this monomer in situ intercalation project, the hypothesis is that intercalation and polymerization will be occurring at the same time. As a result, ZrP/PAM intercalation compound were expected to be formed. The most direct way to analyze the compounds is to de-intercalate the guest compounds and analyze the de-intercalated guests. However, we failed to de-intercalate the guests after many trials. Nevertheless, some indirect characterizations showed evidences which support the formation of PAM within the layers.

A control experiment mimicking the reaction during the in situ synthesis (i.e., hydrothermal treatment of polyacrylamide in the same reaction condition in the presence of H_3PO_4 but in the absence of $ZrOC_{12}$) was conducted to investigate the potential change of acrylamide monomers. Surprisingly, the control sample turned to be gelatineous and

cannot be dissolved in water, which is very different from regular liner PAM. This indicated that the acrylamide was both polymerized and cross-linked. Therefore, there are several possibilities for the intercalated guest: acrylamide monomer, linear PAM, crosslinked PAM, or their combinations. Figure 46 shows the thermogravometric analyses (TGA) testing results. Pure monomer acrylamide starts to lose weight at about 90 °C, and totally decomposed at about 160°C. PAM exhibited several stage of weight loss, while crosslinked PAM mainly lost weight from 180 – 420 °C. The weight loss of the ZrP based intercalation compounds does not match the weight loss of acrylamide at all, but showed a close pattern as the crosslinked PAM. The weight loss of the intercalation compound mainly occurred from 210 – 500 °C, and overall weight loss rate also matches the weight loss weight of the crosslinked PAM (Figure 47). The delayed weight loss compared to the crosslinked PAM can be explained by the bonding energy effect and protection effect by the inorganic layers, which is similar to what happen to ZrP/PEG intercalation compounds as discussed in Figure 40 in Chapter 2. There might be PAM present in the intercalation compounds. However, considering the weight loss of the intercalation compounds after 500 °C was very marginal, which suggested that the concentration of PAM should be very low. At least, the TGA data showed that there is no acrylamide presented in the intercalation compounds, since there was no corresponding weigh losses for acrylamide at ca. 120 – 155 °C observed in the intercalation compound.
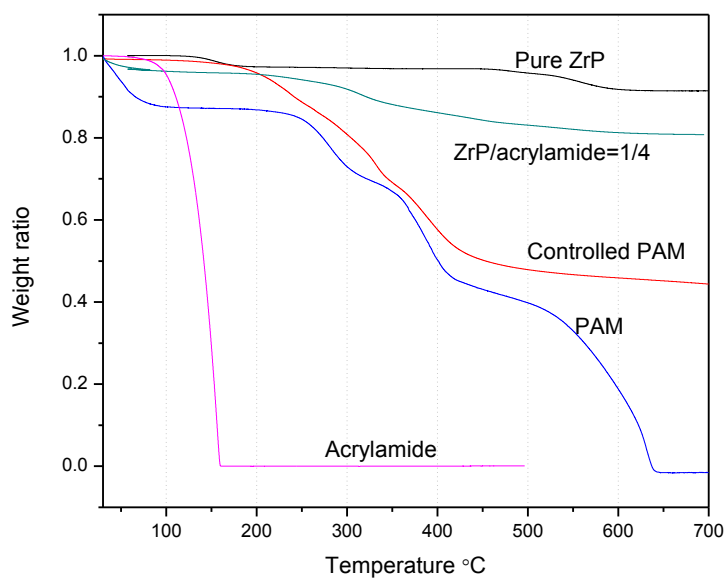
Figure 46. TGA patterns for acrylamide monomer, PAM, controlled PAM,

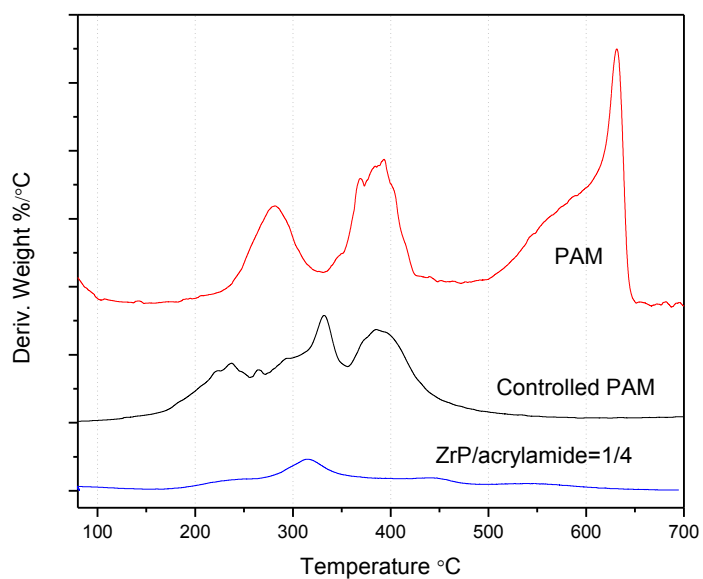ZrP/acrylamide 1:4 ratio, and pure ZrP.

Figure 47. Derivative results of TGA for PAM, controlled PAM, and

ZrP/acrylamide=1/4.

The IR spectra further confirmed the hypothesis that the intercalants are PAM and crosslinked PAM mixture. In Figure 48, to compare acrylamide with the intercalation compound and PAM, one can find that the peak at 1650 cm^{-1}, which is contributed by the C=C double bond,[12] disappeared in the intercalation compounds. Once the acrylamide monomers are polymerized, the C=C double bonds are opened. Thus, PAM should have no peak that represents this double bond. The absence of this peak at 1650 cm^{-1} supported that there is no acrylamide monomers in the intercalation compound, which is consistent with the FTIR results. This evidence, again, supports the hypothesis that acrylamide monomers were polymerized during the synthesis of the intercalation compound in the ZrP interlayer space. The two peaks at 1353 and 1282 cm^{-1} peaks are contributed by NH_2.[83] The entire series of samples in Figure 48 have the 1353 and 1282 cm^{-1} peaks, since the polymerization will not influence the NH_2 group. For the intercalation compound, these two peaks were shifted slightly to low frequencies. This can probably be attributed by the ZrP layers confinement.
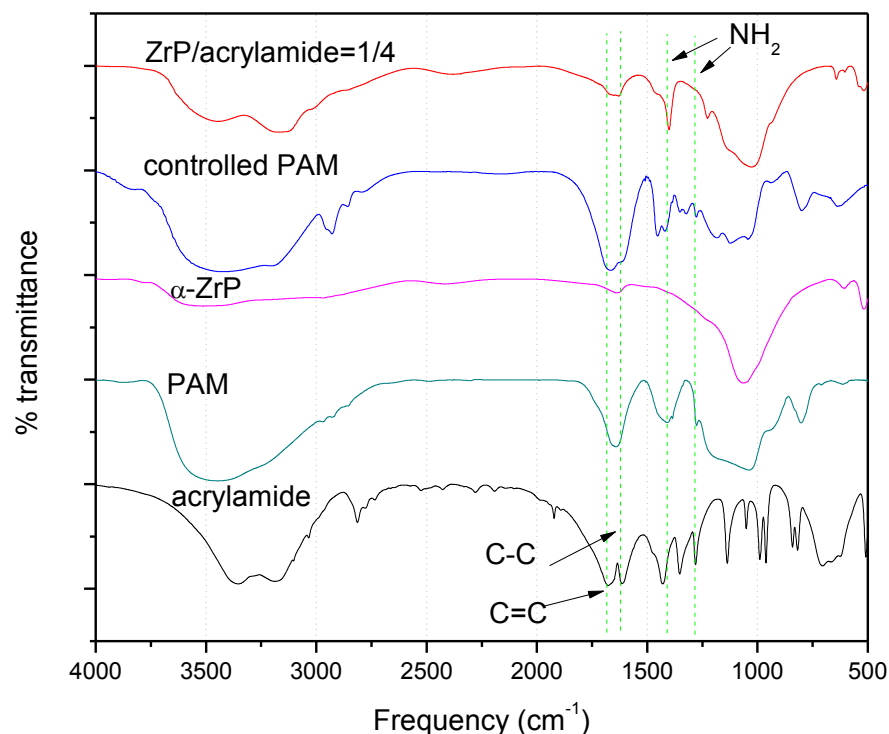
Figure 48. IR spectra for acrylamide, PAM, pure ZrP, controlled PAM and

ZrP/acrylamide=1/4 intercalation compound.

To further prove that acrylamide was embedded into the ZrP layers during the

formation of ZrP crystals and subsequently polymerized, instead of being polymerized

before being intercalated into ZrP, a control experiment was carried out and the results

were shown in Figure 5. A sample of PAM was first synthesized from acrylamide

monomer initiated by ammonium persulfate at room temperature. Polymerized

acrylamide was reacted with $ZrOCl_2$ solution and H_3PO_4 under the same condition to

synthesize the above intercalation compounds. The final product was collected and dried

for XRD. The result showed that no PAM was intercalated into the ZrP. This result

suggested that pre-formed PAM cannot be intercalated under the same condition of *in*

situ synthesis reaction, which in turn suggests that acrylamide were polymerized either during or after the embedding.
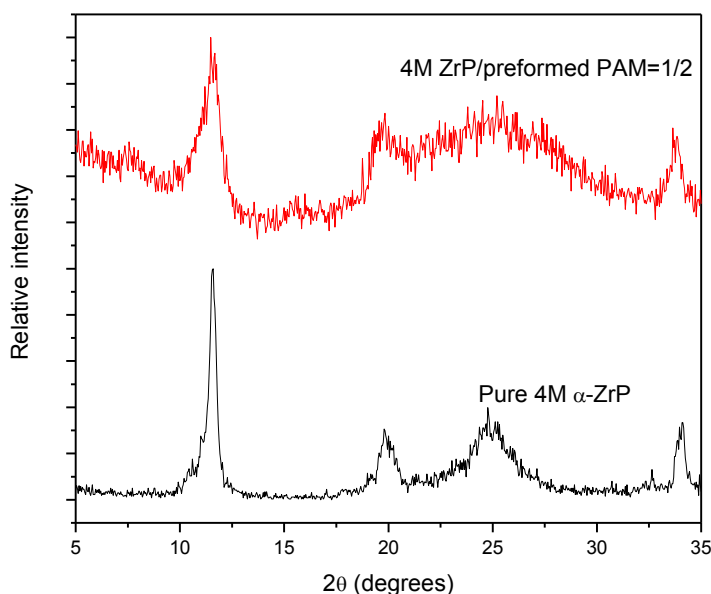

Figure 49. XRD patterns for direct intercalation of 4M ZrP with PAM.

4. Conclusions and future works

The strategy to synthesize layered materials in the presence of polymerizable monomers proved to be successful. Both the TGA and the FTIR results indicated that the intercalants are PAM or crosslinked PAM. Meanwhile, the XRD characterization indicated that it is hard to achieve in situ intercalation using a low concentration of monomers, which is consistent with the results in Chapter 2.

On the other hand, more detailed characterization is to be continued to investigate what is the exact intercalant and related reaction mechanism involved in this in situ reaction in the presence of monomers.

References

1. Bermúdez, R. A.; Colón, Y.; Tejada, G. A.; Colón, J. L., Intercalation and Photophysical Characterization of 1-Pyrenemethylamine in Zirconium Phosphate Layered Materials. Langmuir 2004, 21 (3), 890-895.

2. Troup, J. M.; Clearfield, A., Mechanism of ion exchange in zirconium phosphates. 20. Refinement of the crystal structure of a-zirconium phosphate. Inorganic Chemistry 1977, 16 (12), 3311-14.

3. Marti, A. A.; Colon, J. L., Direct Ion Exchange of Tris(2,2'-bipyridine)ruthenium(II) into an a-Zirconium Phosphate Framework. Inorganic Chemistry 2003, 42 (9), 2830-2832.

4. Kim, H. N.; Keller, S. W.; Mallouk, T. E.; Schmitt, J.; Decher, G., Characterization of zirconium phosphate polycation thin films grown by sequential adsorption reactions. Chemistry of Materials 1997, 9 (6), 1414-1421.

5. Coronado, E.; Marti-Gastaldo, C.; Navarro-Moratalla, E.; Ribera, A.; Galan-Mascaros, J. R., Intercalation of two-dimensional oxalate-bridged molecule-based magnets into layered double hydroxide hosts. Journal of Materials Chemistry 2010, 20 (42), 9476-9483.

6. Messing, R. A., Immobilized enzymes for industrial reactors: New York, 1975.

7. Takei, T.; Kobayashi, Y.; Hata, H.; Yonesaki, Y.; Kumada, N.; Kinomura, N.; Mallouk, T. E., Anodic Electrodeposition of Highly Oriented Zirconium Phosphate and Polyaniline-Intercalated Zirconium Phosphate Films. Journal of the American Chemical Society 2006, 128 (51), 16634-16640.

8. Patro, T. U.; Wagner, H. D., Layer-by-layer assembled PVA/Laponite multilayer free-standing films and their mechanical and thermal properties. Nanotechnology 2011, 22 (45), 455706.

9. Bertrand, P.; Jonas, A.; Laschewsky, A.; Legras, R., Ultrathin polymer coatings by complexation of polyelectrolytes at interfaces: suitable materials, structure and properties. Macromolecular Rapid Communications 2000, 21 (7), 319-348.

10. Lin, J.-J.; Chen, Y.-M.; Yu, M.-H., Hydrogen-bond driven intercalation of synthetic fluorinated mica by poly(oxypropylene)-amidoamine salts. Colloids and Surfaces A: Physicochemical and Engineering Aspects 2007, 302 (1–3), 162-167.

11. Sun, L.; Boo, W. J.; Sue, H.-J.; Clearfield, A., Preparation of α-zirconium phosphate nanoplatelets with wide variations in aspect ratios. New Journal of Chemistry 2007, 31 (1), 39-43.

12. Murugan, S.; Mohan, S.; Bigotto, A. In Polarized Raman and FTIR Spectra of Acrylamide and Polyacrylamide, INTERNATIONAL CONFERENCE ON RAMAN SPECTROSCOPY, JOHN WILEY & SONS LTD: 1996; pp 276-277.

CHAPTER IV

SUMMARY AND FUTURE WORK

Intercalation chemistry has been investigated and developed for over a hundred years. Various intercalation materials have led to widespread application, which has directly or indirectly benefited our daily life and will contribute in more aspects in the future.

The new intercalation strategy, one-pot *in situ* intercalation synthesis, was invented and proved be successful, which were discussed in details in Chapters II and III, respectively. In comparison with the traditional intercalation methodologies, this new strategy provides a new intercalation approach, particularly for those large guest species and/or those guest species lack intercalation driving force to achieve intercalation. As a result, the new intercalation compounds, which were hard or impossible to be synthesized through the conventional intercalation routes, may be synthesized. In addition, since this one-pot *in situ* intercalation synthesis consumes less time and energy and is of lower cost, it holds high promise for commercialization.

So far, the in situ intercalation mechanism and its potential applications have not been completely investigated and clarified, especially for the *in situ* synthesis involves monomers. Various combinations of hosts and guests will be investigated in the future. In addition to 2-D layered materials, 1-D and 3-D host materials, will be explored as well to

synthesize various nanostructured materials. Consequently, the potential applications for this new strategy are very promising. On the other hand, the mechanism for the *in situ* intercalation synthesis must be fully investigated and clarified. It believes that after the complete understanding of the mechanism, more efficient synthesis procedures will be refined, which in turn facilitate to lead to more intercalation applications.

In conclusion, the one-pot *in situ* intercalation compound synthesis method was innovative and proved to be successful by many experiment results. Lots of potential applications will benefit from this new intercalation method. It is very necessary to continue explore its fundamental mechanisms and applications.

VITA

Lichen Xiang was born in Beijing, China, on August 21, 1988, the son of Jian Xiang and Jingnian Xu. After completing his work at Luhe High school, Beijing, China, in 2006, he entered Shanghai Ocean University. He received the degree of Bachelor of Science from Shanghai Ocean University in June 2010. In January 2011, he entered the Graduate College of Texas State University-San Marcos.

Permanent E-mail Address: lincolnhsiang@gmail.com

This thesis was typed by Lichen Xiang.